UPPSALA
UNIVERSITET

UPTECF13031
Examensarbete 30 hp
16 September 2013

Estimation of heading using magnetometer and GPS

Manne Henriksson

UPPSALA
UNIVERSITET

Teknisk- naturvetenskaplig fakultet
UTH-enheten

Besöksadress:
Ångströmlaboratoriet
Lägerhyddsvägen 1
Hus 4, Plan 0

Postadress:
Box 536
751 21 Uppsala

Telefon:
018 – 471 30 03

Telefax:
018 – 471 30 00

Hemsida:
http://www.teknat.uu.se/student

Abstract

Estimation of heading using magnetometer and GPS

Manne Henriksson

One important part of inertial navigation is the estimation of the direction relative to the Earth's geographic North Pole, the so called heading. In this project, a gyroscope and an accelerometer were used together in an Extended Kalman Filter with a quaternion as the state space variable, representing the attitude. Given the attitude of the system, measurements from a magnetometer were rotated to a horizontal coordinate frame in order to calculate the direction toward Earth's magnetic North Pole. Comparing this direction with the angle toward the Geographic North Pole given by a GPS, the local magnetic declination was estimated with the purpose of correcting the heading in the future. Different methods for detecting disturbances on the magnetometer in order to automatically decide when it is to be trusted was discussed and evaluated. Routines for easily performing sensor calibration was created. The outcome of the project was a well working attitude estimation, simply performed calibration routines and a set of methods working together to detect magnetometer disturbances.

Handledare: Daniel Hellberg
Ämnesgranskare: Tomas Olofsson
Examinator: Tomas Nyberg
ISSN: 1401-5757, UPTEC F13 031

Estimation of heading using magnetometer and GPS

Manne Henriksson

September 16, 2013

Abstract

One important part of inertial navigation is the estimation of the direction relative to the Earth's geographic North Pole, the so called heading. In this project, a gyroscope and an accelerometer were used together in an Extended Kalman Filter with a quaternion as the state space variable, representing the attitude. Given the attitude of the system, measurements from a magnetometer were rotated to a horizontal coordinate frame in order to calculate the direction toward Earth's magnetic North Pole. Comparing this direction with the angle toward the Geographic North Pole given by a GPS, the local magnetic declination was estimated with the purpose of correcting the heading in the future. Different methods for detecting disturbances on the magnetometer in order to automatically decide when it is to be trusted was discussed and evaluated. Routines for easily performing sensor calibration was created. The outcome of the project was a well working attitude estimation, simply performed calibration routines and a set of methods working together to detect magnetometer disturbances.

Contents

Acronyms

GPS	Global Positioning System
INS	Inertial Navigation System
ZUPT	Zero-Velocity-Update
RFID	Radio Frequency Identification
IMU	Inertial Measurement Unit
DCM	Direction Cosine Matrix
EKF	Extended Kalman Filter

Chapter 1

Introduction

1.1 Background

Navigation is today commonly done by using the Global Positioning System (GPS). If however the GPS signal is disturbed or not present at all, navigation using only a GPS will not be successful. In these situations, sensors such as a gyroscope, an accelerometer and a magnetometer can give useful information. Combining such sensors for navigation can form an Inertial Navigation System (INS).

The main drawback with an INS is the lack of absolute reference. If the sensors are not perfect, errors will accumulate resulting in a drift in position with no possibility to reset to the correct position. Considering the weaknesses for both the GPS and the INS, it seems advantageous to combine the two to form a more reliable navigation system. Such system could be attached to different types of vehicles such as cars and airplanes. In this thesis however, only navigation performed by a human will be considered and thus the sensors will be attached to a human body.

The work done in this project covers one important part of a man carried INS: the heading estimation, i.e., the estimation of the angle between the torso of the body and the geographic North Pole.

1.2 Related work

Many solutions for navigation using a man carried INS use foot mounted sensors. One benefit with attaching the sensors to one of the persons feet is that the Zero-Velocity-Update (ZUPT) strategy [3] can be used. In many situations, updating the position by simply integrating the measurements from the accelerometer twice will work badly since measurement noise accumulates quickly. The main idea of the ZUPT technique is to use the fact that the velocity of the foot is zero when it is in contact with the ground during a step. This fact can be used in order to reset the velocity to zero in each step and thereby avoiding the accumulation of error in the velocity estimation. The sensors used in this project will however be attached to the torso of the body and the ZUPT strategy will therefore not be used. The reason for this choice of sensor placement is that attaching the sensors to the persons feet would require cables to be drawn from the feet to the upper parts of the body, which preferably is avoided for the specific application intended.

Another approach for inertial navigation is to estimate the frequency at which the person

is taking steps, the length of the steps and the direction in which the person is facing, i.e., the heading. For determining the heading, which is the aim of the project covered in this thesis, a gyroscope, an accelerometer and a magnetometer will be used. Measurements from these sensors can be combined in many different ways. This is typically done by a state variable representing the so called attitude of the system, i.e. the orientation of the system about its center of mass. The attitude can be expressed in a number of different ways. One alternative is to represent it in the classic and intuitive way by defining three angles under which the system has rotated relative to some coordinate frame. Typical conventions in the defense industry are to use the Euler angles yaw, pitch and roll or heading, elevation and bank. Another common way to represent the attitude is to make use of so called quaternions [12], [13].

The different types of sensors can be used together in different ways in order to keep track of the attitude. One way is to use all sensors to update the state variable and calculating the heading directly from this as in [10]. Another approach is to first use the gyroscope and accelerometer to estimate the attitude and then use this information for transforming the magnetometer data in order to calculate the heading from this.

When using the accelerometer for updating the attitude, the measured acceleration vector is interpreted as the Earth's gravity vector measured in the coordinate frame of the sensors. If the sensors are accelerating, the measurements from the accelerometer will contain this acceleration in addition to the Earth's gravity vector. Such acceleration is often referred to as external acceleration. The problem is handled in [10] and [11] by adjusting how much the system trusts the accelerometer depending on the direction and the amount of the external acceleration. Another method for compensating for external acceleration is to derive the acceleration of the body from GPS signals as done in [14]. In that paper however, the attitude system is intended for a car, which will have larger and less noisy accelerations than in this thesis and therefore the acceleration from GPS data is more useful. Navigation on the Earth involves acceleration not only from the body itself but also from the movement of the planet. The angular velocity from the rotation of the planet can be felt by a really good gyroscope. If the body is moving quickly, the tangent plane to the earth will rotate as the body translates which can also be detected by the gyroscope. These problems are faced in [15] for an airplane application.

A common problem using inertial navigation, regardless of if the ZUPT strategy or the step length, step frequency and heading approach is used, is that the error in position will accumulate unless an update of the absolute position can be performed. This can be done by using a GPS as in [15]. If the navigation is to be performed indoors or among tall buildings or other obstacles, signals from the GPS, if even present, will be corrupted. If the navigation is to be performed in beforehand known buildings, checkpoints or landmarks can be put at strategic positions in order to be able to reset the position. This is done in [19] by using Radio Frequency Identification (RFID) tags, placed at different places in the building. If the navigation system has the ability to sense wi-fi access, this can be used for position reference as in [20], where also positions that exhibit specific features, such as elevators, are considered. The navigation considered in this thesis is to be performed in unknown areas and buildings and therefore approaches using landmarks cannot be used.

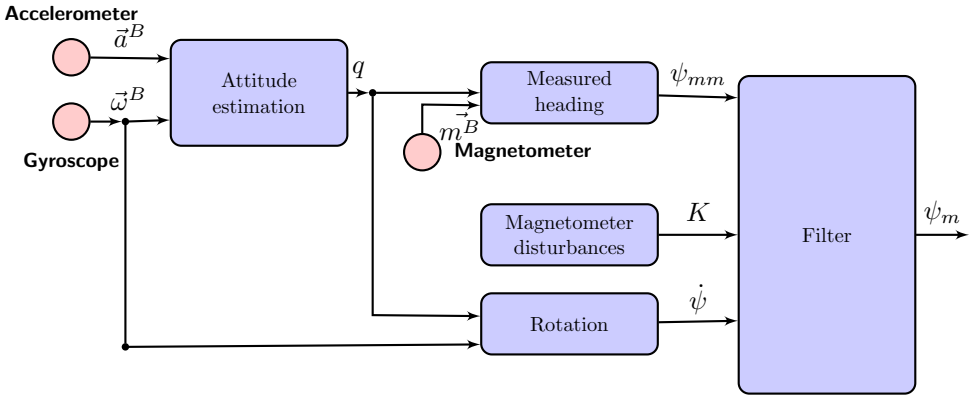

Figure 1.1: The subsystem considered in this thesis. Input is sensor data from accelerometer, gyroscope and magnetometer and output is the magnetic heading.

1.3 Problem formulation

The goal of the project covered in this report is to find the heading for a man carried INS. The heading can be thought of as the angle between the direction in which the person is facing and the direction toward the geographical North Pole. The direction toward the magnetic North Pole can easily be calculated by using a magnetometer for measuring the magnetic field vector in the horizontal plane, as one would do with a compass. This would work fine if the person carrying the INS would always stand in an upright position. This is unfortunately not the case, since even by just walking, the sensor axes will be tilted relative to the horizontal plane and extracting the horizontal component of the magnetic field from the sensor axes will not be as trivial. However, if the rotation of the sensors relative to the horizontal plane is known, this information can be used in order to extract the horizontal component from the magnetometer data. Therefore, this rotation, known as the attitude, must always be known.

The magnetometer may be disturbed by other magnetic fields than the Earth's and automatically detecting whether the magnetometer is being disturbed or not is therefore important. If the heading is used in an INS that is to be used in a fusion with data from a GPS, the direction toward the geographical North Pole and not the magnetic North Pole must be known. This difference is called the declination and is in this project estimated by comparing the heading calculated from the magnetometer with that calculated from a GPS. Finally, calibrating the sensors before use is essential in order to get useful information from them.

1.4 System overview

An overview of the most important parts of the proposed solution for the heading estimation in this thesis can be seen in figure 1.1. Starting from the right side in the figure, the direction toward the Earth magnetic North Pole, ψ_m, is calculated using a fusion of the measured heading from the magnetometer, ψ_{mm}, and the rate of change of the heading measured by the gyroscope, $\dot{\psi}$. This fusion will weight the sensor measurements different depending on the presence of disturbances on the magnetometer and this weighting is represented by K in the figure. Since ψ_m will be the angle toward the Earth's magnetic North

pole and not the geographic one, this angle will be referred to as the magnetic heading. When the effect of the declination is added to ψ_m, the result is the heading, denoted ψ. The rate of change of the heading, $\dot{\psi}$, is the same regardless of if the magnetic heading or the heading is considered, since these two only differs by a constant offset. The measured heading from the magnetometer, ψ_{mm} will be referred to as the measured heading.

Most of the techniques for detecting the disturbances on the magnetometer are subject to patent pending at the company where the project was performed. Because of this, not much will be said about these techniques and the part "Magnetometer disturbances" in the figure does therefore not have any input.

The measured heading and the velocity of the heading will be calculated from the magnetometer and the gyroscope respectively. These sensors will rotate with the body of the person to which they are attached and therefore these calculations will not be trivial. Because of this, the attitude, i.e. the rotation of the system relative to some starting orientation must constantly be known. Information about the attitude is then used in order to rotate the sensor data such that they can be used as if no rotation had been performed. The estimation of the attitude can be seen to the left in the system overview figure and it uses the accelerometer data $\vec{a}^B$ and the gyroscope data $\vec{\omega}^B$ in order to estimate the attitude denoted by q in the figure. The index B indicates that the measurements are represented in a coordinate system fixed to the body.

The accelerometer and the gyroscope have strengths and weaknesses that make them good complements to each other. The gyroscope is good at detecting short term changes in the attitude but inevitably looses the correct value of the attitude after some time due to measurement noise. The accelerometer on the other hand, compares the measured acceleration vector with Earth's gravity vector and can therefore give information about the attitude no matter how much time has passed since the true attitude was known. An instantaneous measurement from the accelerometer might however be very corrupted regarding the attitude, since the measured acceleration might come from body movement and not from the Earth's gravity vector. When the attitude is known, it can be used in order to rotate the measurements from the gyroscope $\vec{\omega}^B$ and the magnetometer $\vec{m}^B$ such that they can be used for extracting the measured heading and the velocity of the heading.

There are two parts covered in this thesis not shown in figure 1.1. The first one is the calibration of the sensors which must be performed in order to get useful measurements from them. The second one is the impact of the declination, i.e, the fact that the magnetometer only can measure the direction toward the Earth's magnetic North Pole and not the geographic North Pole. This will be solved by detecting the difference between the two by comparing the direction toward the magnetic north calculated from the magnetometer with the direction toward the geographic north calculated from the GPS, given that both can be estimated correctly.

1.5 Thesis organization

Including this chapter, the thesis contains 8 chapters with the following content:
Chapter 2 contains the theory that will be used throughout the thesis. Some of the mayor topics covered are different types of filters, coordinate frames and the relationship between them. Different types of representation of the attitude, especially quaternions,

are thoroughly covered.
Chapter 3 treats the attitude system. The chapter explains how the gyroscope and the accelerometer are used together to estimate the attitude. Extreme rotations that causes the definition of the heading to be misleading are treated by the introduction of an alternative definition of the heading in such situations. The external accelerations which cause the accelerometer measurements to be misleading are also handled in this chapter.
Chapter 4 discusses methods for how the fusion between the measured heading and the velocity of the heading is performed in order to calculate the magnetic heading. This chapter is not complete in this report due to a pending patent, but one method that uses the strength of the magnetic field to adjust the weighting in the fusion is introduced.
Chapter 5 explains how the magnetic declination is estimated by comparing the magnetic heading with the course given by a GPS.
Chapter 6 shows the results for the different parts of the project.
Chapter 7 contains a few conclusions, a discussion about the project and some ideas for further work.

Chapter 2

Theory

All theory used in the proceeding chapters will be introduced in this chapter. First, the Extended Kalman Filter (EKF), which is used as a filter in the attitude estimation, will be explained. Next, a simple digital low pass filter will be explained since it will be used for filtering both for the accelerometer data in chapter 3 and the magnetometer data in chapter 4. After that, a brief explanation of the sensors will be done followed by the definitions of some important coordinate frames, which must be considered when rotating the measurement data and calibrating the sensors. Next, the mathematics behind spatial rotation is introduced since it will be used for rotating the measurement data. A quaternion will be used for representation of the attitude system and therefore a motivation of why and some quaternion theory follows next. Finally, theory necessary for describing the calibration of the sensors will be presented.

2.1 The Kalman filter

2.1.1 State space model

A state space model will be used in this thesis to model the attitude. The measurements of the attitude system will be made in discrete time, since they are discrete samples from the accelerometer and the gyroscope. A linear state space model in discrete time commonly used in signal and control applications is:

$$x_{k+1} = F_k x_k + w_k \tag{2.1a}$$

$$z_k = H_k x_k + v_k \tag{2.1b}$$

where k indicates the time instance, x_k is an n-dimensional vector representing the state variable, F_k is an n by n matrix, z_k is an m-dimensional vector representing the measurement of the system, H_k is an m by n matrix and w_k and v_k are uncorrelated white noise with covariance matrices:

$$E\{w_k w_{k+l}^T\} = Q_k \delta_0[l] \tag{2.2a}$$

$$E\{v_k v_{k+l}^T\} = R_k \delta_0[l], \tag{2.2b}$$

where l is an arbitrary integer and $\delta_0[l]$ is the Kronecker delta function:

$$\delta_0[l] = \begin{cases} 1 & \text{if } l = 0 \\ 0 & \text{else.} \end{cases} \tag{2.3}$$

2.1.2 The Kalman equations

Given the linear state space model in equation 2.1 and the conditions in equation 2.2, the Kalman filter is the best possible estimator of the state variable among all linear ones [24]. The goal is to estimate the state space variable x and its error covariance matrix, P, representing the uncertainty in the estimation. The state vector x and the covariance matrix P need to be initialized and these values are denoted x_0 and P_0. Since the output from the Kalman filter is an estimate of the state, the variable representing the state is given a hat symbol such that this estimate, $\hat{x}$, is easily distinguished from the true value, x. The Kalman filter can be thought of as working in two distinct phases: the predict phase and the update phase. In order to distinguish between the different phases the state variable and the error covariance matrix will be given two subindexes representing when the estimation is done and which measurements the estimation is based on. For instance, the state variable $\hat{x}_{a|b}$ means the estimation of x at time instance a based on all measurements up to time instance b.

Prediction:

$$\hat{x}_{k|k-1} = F_k \hat{x}_{k-1|k-1} \tag{2.4a}$$

$$P_{k|k-1} = F_k P_{k-1|k-1} F_k^T + Q_k \tag{2.4b}$$

Update:

$$\hat{x}_{k|k} = \hat{x}_{k|k-1} + K_k(z_k - H_k \hat{x}_{k|k-1}) \tag{2.5a}$$

$$P_{k|k} = (I - K_k H_k) P_{k|k-1}, \tag{2.5b}$$

where K_k is the Kalman gain given by:

$$K_k = P_{k|k-1} H_k^T (H_k P_{k|k-1} H_k^T + R_k)^{-1} \tag{2.6}$$

and $\hat{x}_{k-1|k-1}$ and $P_{k-1|k-1}$ are the state variable and the covariance matrix from the previous time instance, $\hat{x}_{k|k-1}$ and $P_{k|k-1}$ are the state variable and the covariance matrix received from the prediction step, while $\hat{x}_{k|k}$ and $P_{k|k}$ will be passed on to next time instance.

2.2 The Extended Kalman filter

A generalization of equation 2.1 can be made by replacing the linear terms $F_k x_k$ and $H_k x_k$ by the potentially nonlinear functions $f[x_k, k]$ and $h[x_k, k]$ respectively. A linear relationship between x_k and x_{k-1} and between x_k and z_k is no longer assumed and the standard Kalman filter cannot be used. Therefore the EKF will be derived for a system of the form:

$$x_{k+1} = f[x_k, k] + w_k \tag{2.7a}$$

$$z_k = h[x_k, k] + v_k, \tag{2.7b}$$

where w_k and v_k are again mutually uncorrelated white noise sequences with covariance matrices Q_k and R_k respectively. The equations for the EKF are:

Prediction:

$$\hat{x}_{k|k-1} = f[\hat{x}_{k-1|k-1}, k] \tag{2.8a}$$

$$P_{k|k-1} = F[k, \hat{x}_{k-1|k-1}] P_{k-1|k-1} F^T[k, \hat{x}_{k-1|k-1}] + Q_k \tag{2.8b}$$

Update:

$$\hat{x}_{k|k} = \hat{x}_{k|k-1} + K_k[z_k - h[\hat{x}_{k|k-1}, k]] \tag{2.9a}$$

$$P_{k|k} = P_{k|k-1} - K_k H[k, \hat{x}_{k|k-1}] P_{k|k-1} \tag{2.9b}$$

where

$$K_k = P_{k|k-1} H^T[k, \hat{x}_{k|k-1}] \{H[k, \hat{x}_{k|k-1}] P_{k|k-1} H^T[k, \hat{x}_{k|k-1}] + R_k\}^{-1} \tag{2.10}$$

is the Kalman gain and

$$H[k, \hat{x}_{k|k-1}] = \frac{\partial h[x, k]}{\partial x}\Big|_{x=\hat{x}_{k|k-1}} \tag{2.11}$$

$$F[k, \hat{x}_{k-1|k-1}] = \frac{\partial f[x, k]}{\partial x}\Big|_{x=\hat{x}_{k-1|k-1}} \tag{2.12}$$

and $\hat{x}_{k-1|k-1}$ and $P_{k-1|k-1}$ are the state variable and the covariance matrix from the previous time instance, $\hat{x}_{k|k-1}$ and $P_{k|k-1}$ are the estimates of the state variable and the covariance matrix received from the prediction step, while $\hat{x}_{k|k}$ and $P_{k|k}$ will be passed on to next time instance. The estimate of the state variable $\hat{x}$ is an n-dimensional vector and the measurement of the system, z, is an m-dimensional vector. The functions f and h are both vector valued functions which ranges are an n-dimensional vector and an m-dimensional vector respectively. The Jacobian H is of dimension n by n and the Jacobian F is of dimension m by n. The error covariance matrix P is of dimension n by n. Both the estimate of the state variable and the error covariance matrix need to initialized and these values are denoted x_0 and P_0 respectively.

2.3 Digital low pass filter

Given a sampled signal $x[k]$ and the desire to low-pass filter this signal to get the signal $y[k]$, a simple model would be:

$$y[k] = \alpha y[k-1] + (1-\alpha)x[k]. \tag{2.13}$$

Taking the z-transform and rearranging the factors gives:

$$H[z] = \frac{Y[z]}{X[z]} = \frac{1-\alpha}{1-\alpha z^{-1}} \tag{2.14}$$

with $H[z]$ representing the transfer function. A common feature in order to compare low pass filters is the time constant, τ, which is defined as the time it takes for the output $y[k]$ to reach the value $1 - \frac{1}{e}$ given that the input signal $x[k]$ is a step function having the z-transform $X[z] = \frac{1}{1-z^{-1}}$. Filtering in time domain corresponds to a multiplication in z-domain, resulting in:

$$Y[z] = H[z]X[z] = \frac{1-\alpha}{1-\alpha z^{-1}} \frac{1}{1-z^{-1}} = \frac{1}{1-z^{-1}} - \frac{\alpha}{1-\alpha z^{-1}}. \tag{2.15}$$

Taking the inverse z-transform gives for $k \geq 0$

$$y[k] = 1 - \alpha^{k+1}. \tag{2.16}$$

Finally setting $y[k]$ equal to $1 - \frac{1}{e}$ and using the relation $\tau = kT_s$ for sample time T_s gives:

$$\alpha = e^{-\frac{T_s}{\tau + T_s}}. \tag{2.17}$$

2.4 The sensors

The sensors used in this thesis are a gyroscope, an accelerometer and a magnetometer. Each sensor will have three axes, an x-axis, an y-axis and a z-axis that optimally are orthogonal to each other. Each sensor will have its x-axis pointing in the same direction as the other sensors x-axis and the same will be true for the y-axes and the z-axes. The gyroscope measures angular velocity with the unit $[1s^{-2}]$, where the actual angle is dimensionless, but can be expressed in radians or degrees. From here on, it will be assumed that the unit is $[1rad/s^2]$.

Generally a gyroscope is based on the fact that a body, typically a disc, rotating around an axis reacts on an external torque around a second axis (generated by some movement of the body) by a rotation around a third axis. By measuring this rotation, or the torque needed to compensate for it, the angular velocity around the second axis will be given. This fact is useful in this project, since the gyroscope can then measure the direction and the magnitude of the angular velocity generated by the body movements, such that the velocity of the heading can be extracted. An accelerometer measures acceleration with the unit $[1m/s^2]$. An accelerometer that is not subject to any forces, for instance in outer space, will measure $0m/s^2$. If an accelerometer is at rest somewhere on the surface of the earth however, it will still measure the Earth gravity g. Finally, a magnetometer measures the strength of a magnetic field and the unit used in this thesis will be Tesla, $[1T]$. The magnetic field is often the Earth's magnetic field, but can also be other fields generated by electronic devices or ferromagnetic material.

2.5 Coordinate Systems

The measured quantities in an INS will be given in a coordinate system that coincides with the axis of the measuring sensors. Since the position given by the INS is to be compared to that from the GPS, it is obvious that some coordinate transformation has to be done. Here follows a description of the coordinate systems, or reference frames, used in this thesis.

2.5.1 Platform frame

The platform frame is a coordinate system coinciding with the sensors of the INS. Each type of sensor (accelerometer, magnetometer and gyroscope) has its own platform frame. The platform frame for each sensor has its x, y and z axis coinciding with the axes along which the measurements are done. Optimally the platform frame for each sensor would coincide with each other and each axis would be orthogonal to the others. For now however, neither will be assumed.

2.5.2 Body frame

The body frame will in this thesis be defined as a coordinate system associated with a box containing the sensors, hereafter referred to as the the Inertial Measurement Unit (IMU). The coordinate axes coincide with the orthogonal sides of the rectangular IMU and when mounted correctly on a person standing up, the x-axis points forward, the z-axis points down and the y-axis completes the right hand rule. The heading angle, which is the main goal of this thesis can be defined in the body frame as:

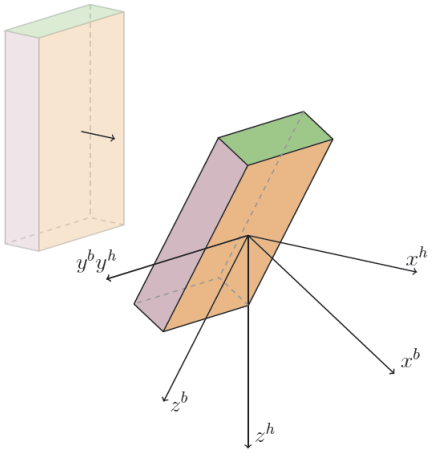

Figure 2.1: The IMU has been rotated around the y-axis. The body coordinates are denoted by index b and the horizontal coordinates by h

Definition 2.5.1. *The **heading** ψ, is the angle between the projection of the x-axis to the horizontal plane and the geographic North Pole of the Earth, such that $\psi \in (-180°, 180°]$. The angle is positive if the projection of the x-axis is pointing to the right of north and negative if it points to the left of north.*

It is not clear from the definition what will happen in situations when the x-axis is orthogonal to the horizontal plane or when the origin of the body frame coincides with the geographic North Pole. The first situation is handled in section 3.3, while the second one is ignored, since it is unlikely it will ever occur. A typical situation can be seen in Figure 2.1, where the body coordinate axes are x^b, y^b and z^b. To calculate the heading, x^b is projected to the horizontal plane resulting in x^h. The heading is then given by the angle between x^h and north.

2.5.3 Inertial frame

An inertial frame is a coordinate system either at rest or in linear motion, such that Newton's laws apply. Preferably, the origin is chosen to coincide with the center of the Earth and its three axes can point in any three mutually orthogonally directions.

2.5.4 Local geodetic frame

The local geodetic frame is an orthogonal Cartesian coordinate system where the x-axis points north, the y-axis east and the z-axis completing the right hand rule pointing down. The z-axis might however not point exactly at the center of Earth, since the planet is not perfectly spherical.

2.6 Rotation sequences

In order to transform the measured quantities from the sensors of the IMU to the different coordinate frames in the previous section, the relationship between them has to be investigated. The Swiss mathematician Leonhard Euler(1707-1783) stated [17]:

Any two independent orthogonal coordinate frames can be related by a sequence of rotations (not more than three) about a coordinate axis, where no two successive rotations may be about the same axis.

The word *related* means that the two coordinate frames coincide. The angle of rotation around a coordinate axis is often referred to as an *Euler angle* and a sequence of such rotations as an *Euler angle sequence*. Such sequence of rotations is often denoted by the three axes around which the rotations are performed, written from left to right in order of rotation. For instance, a rotational sequence xyz means a rotation around the x-axis followed by a rotation around the y-axis followed by a rotation around the z-axis. There are in fact 12 possible rotation sequences all fulfilling the requirements stated by Euler. The rotation sequence most commonly used in aircraft and aerospace applications, and therefore used in this thesis, is the zyx sequence. In aerospace applications, the body frame is a coordinate system with origin at the center of mass of the aircraft with its x-axis pointing forward, the y-axis along the right wing and the z-axis completing the right hand rule. For the application in this thesis, the body frame is similar with the origin at the center of mass of the IMU, the x-axis pointing forward and the y-axis to the persons right. The transformation from the local geodetic frame to the body frame is performed by the zyx sequence in the following order:
- A rotation of an angle $\psi \in (-180, 180]$ around the z-axis defining the heading.
- A rotation of an angle $\theta \in [-90, 90]$ around the y-axis defining the pitch.
- A rotation of an angle $\phi \in (-180, 180]$ around the x-axis defining the roll.

A rotation of an n-dimensional vector $\mathbf{v}$ can be described mathematically by pre-multiplying it by with an n by n matrix M. The result is a new n-dimensional vector $\mathbf{u}$, such that $\mathbf{u} = M\mathbf{v}$. If M^x,M^y and M^z denotes the rotation around the x-axis, y-axis and z-axis respectively, the rotation matrix from body frame to local geodetic frame $M_b^l = M^x M^y M^z$ becomes:

$$M_b^l = \begin{pmatrix} cos\psi cos\theta & sin\psi cos\theta & -sin\theta \\ cos\psi sin\theta \sin\phi - sin\psi cos\phi & sin\psi sin\theta sin\phi + cos\psi cos\phi & cos\theta sin\phi \\ cos\psi sin\theta cos\phi + sin\psi sin\phi & sin\psi sin\theta cos\phi - cos\psi sin\phi & cos\theta cos\phi \end{pmatrix} \tag{2.18}$$

since

$$M^z = \begin{pmatrix} cos\psi & sin\psi & 0 \\ -sin\psi & cos\psi & 0 \\ 0 & 0 & 1 \end{pmatrix} \tag{2.19a}$$

$$M^y = \begin{pmatrix} cos\theta & 0 & -sin\theta \\ 0 & 1 & 0 \\ sin\theta & 0 & cos\theta \end{pmatrix} \tag{2.19b}$$

$$M^x = \begin{pmatrix} 1 & 0 & 0 \\ 0 & cos\phi & sin\phi \\ 0 & -sin\phi & cos\phi \end{pmatrix}. \tag{2.19c}$$

The relationship between a vector represented in the body frame $\mathbf{u}^b = x\mathbf{u}_1 + y\mathbf{u}_2 + z\mathbf{u}_3$ is thus related to a vector in the local geodetic frame $\mathbf{v}^l = n\mathbf{v}_1 + e\mathbf{v}_2 + d\mathbf{v}_3$ (north, east, down) as $\mathbf{v}^l = M_b^l \mathbf{u}^b$. The vectors $\mathbf{u}_1, \mathbf{u}_2$ and $\mathbf{u}_3$ are orthogonal unit vectors spanning the body frame and the vectors $\mathbf{v}_1, \mathbf{v}_2$ and $\mathbf{v}_3$ are orthogonal unit vectors spanning the local geodetic frame. As can be seen in equation 2.18, M_b^l is itself a 3 by 3 matrix corresponding to a single rotation. A useful property of a rotation matrix M is the fact that its inverse

is equal to its transpose, i.e., $M^{-1} = M^T$.

The rotation matrix is also known under the name transformation matrix or Direction Cosine Matrix (DCM). The latter name comes from the fact that each element m_{ij} in M_b^l is the direction cosine relating $\mathbf{u}_j$ to $\mathbf{v}_i$. The direction cosine between two vectors is the cosine value of the angle between them or, since both of them are of unit length, the scalar product between them. It is important to note, that using any of the Euler sequences possible for the specific rotation (using the necessary values for the angles) would give the same rotation matrix. This can be intuitively explained by thinking of the rotation matrix as the DCM, representing the angles between the unit vectors of the reference frames. It is obvious that no matter in what order the rotations were performed, these values should be the same. With this in mind, it can be useful to calculate the *zyx*-Euler angles, given only the rotation matrix. By using the relationship in equation 2.18 between ψ, θ and ϕ and some of the elements m_{ij} of M, we get:

$$\psi = atan2(m_{1,2}, m_{1,1}) \tag{2.20a}$$
$$\theta = asin(-m_{1,3}) \tag{2.20b}$$
$$\phi = atan2(m_{2,3}, m_{3,3}) \tag{2.20c}$$

where $atan2(x, y)$ is the same as $atan(\frac{x}{y})$ but unambiguous regarding the quadrant. Now, let's say that the attitude of a system is to be modeled by these three Euler angles as the variable in a state space model and that a three-axis gyroscope is used for updating the variable. The relation between the derivative of the angles and the angles are then given by:

$$\begin{pmatrix} \dot{\psi} \\ \dot{\theta} \\ \dot{\phi} \end{pmatrix} = \begin{pmatrix} 0 & \frac{sin(\phi)}{cos(\theta)} & \frac{cos(\phi)}{cos(\theta)} \\ 0 & cos(\phi) & -sin(\phi) \\ 1 & tan(\theta)sin(\phi) & tan(\theta)cos(\phi) \end{pmatrix} \begin{pmatrix} \omega_x \\ \omega_y \\ \omega_z \end{pmatrix}. \tag{2.21}$$

Here ω_x, ω_y and ω_z are the measured angular velocities around the three axes. As can be seen, two elements in the matrix contain the term $cos(\theta)$ in the denominator. If $\theta = \pm 90°$, then these elements involves a division by 0. This is commonly known as a *gimbal lock*. The system would also be unstable for values of θ close to $\pm 90°$, since this would involve a division by a potentially very small number. For these reasons, the Euler angles will not be used for representing the attitude in this project. In order to get to the representation used, another famous theorem by Euler [18], related to the first one is presented. It states the fact that the consecutive rotations can be represented by a single one:

In whatever way a sphere might be rotated around its own center, a diameter can always be chosen whose direction in the rotated configuration would coincide with the original configuration.

This theorem offers the possibility to instead of representing the rotation by the three angles ψ, θ and ϕ, represent it by the axis of rotation and the angle of rotation around this axis. Using unit quaternions offers a mathematically simple but less intuitive representation that avoid the singularities in equation 2.21 and it will be presented in the next section.

2.7 Quaternions

The quaternion will be used for describing the rotation matrix between the body coordinate frame and the local geodetic frame. However, before specifically describing the practical aspects, some mathematical background will be presented.

2.7.1 History and definition

The quaternion was discovered by the Irish mathematician Sir William Rowan Hamilton (1805-1865) in 1840 when he was looking for a way to extend the complex numbers to higher dimensions. The event is famous since the solution hit him suddenly while he was out walking with his wife. In the side of Broom Bridge in Dublin, he carved with his penknife:

$$i^2 = j^2 = k^2 = ijk = -1. \tag{2.22}$$

A complex number can be said to have rank 2, a pure real part and a pure imaginary part. A quaternion is a hyper-complex number of rank 4, with 3 imaginary parts and 1 real part. The imaginary parts are i, j and k, satisfying the relationships in equation 2.22. The quaternion can now be defined:

Definition 2.7.1. *A quaternion q is the sum of a vector in R^3 and a scalar.*
$q = q_0 + \boldsymbol{q} = q_0 + \boldsymbol{i}q_1 + \boldsymbol{j}q_2 + \boldsymbol{k}q_3$.

The variable q_0 will be called the scalar part and $\mathbf{q}$ the vector part. The variables q_0, q_1, q_2 and q_3 are all scalars. The vectors $\mathbf{i}$, $\mathbf{j}$ and $\mathbf{k}$ together spans R^3 and can be written as

$\mathbf{i}$ = (1,0,0)
$\mathbf{j}$ = (0,1,0)
$\mathbf{k}$ = (0,0,1)

As will be seen in section 2.7.2, the quaternions used for spatial rotation have the additional requirement that they have norm 1, i.e. they are unit quaternions.

Definition 2.7.2. *A unit quaternion is a quaternion $q = q_0 + \boldsymbol{q}$ with the additional requirement $q_0^2 + |\boldsymbol{q}|^2 = 1$.*

An important property for the quaternion, following directly from the definition, is that multiplication is not commutative. The following table shows the result of multiplying two vectors:

$$\begin{aligned} ij &= k, \quad ji = -k \\ jk &= i, \quad kj = -i \\ ki &= j, \quad ik = -j \end{aligned} \tag{2.23}$$

The complex conjugate of a quaternion is important for the applications in this thesis and must therefore be defined:

Definition 2.7.3. *The* complex conjugate *of a the quaternion $q = q_0 + \boldsymbol{q}$ is a quaternion denoted q^*, given by $q^* = q_0 - \boldsymbol{q}$.*

It can easily be proven that $\sqrt{q^*q} = \sqrt{q_0^2 + q_1^2 + q_2^2 + q_3^2} = |q|$.

2.7.2 Connection to spatial rotation

For a unit quaternion, by the definition,

$$q_0^2 + |\mathbf{q}|^2 = 1. \tag{2.24}$$

For any angle θ, the relation $\cos^2\theta + sin^2\theta = 1$ holds. Now since $q_0^2 \leq 1$, there must be some angle θ such that

$$cos^2\theta = q_0^2 \tag{2.25a}$$

and

$$sin^2\theta = |\mathbf{q}|^2. \tag{2.25b}$$

Under the restriction: $-\pi < \theta < \pi$, the angle θ is uniquely defined and associated with the quaternion q. The relation can therefore be written:

$$q = cos\theta + \mathbf{u}sin\theta \tag{2.26}$$

where $\mathbf{u}$ is a unit vector. If θ defines an angle of rotation around the axis defined by the unit vector $\mathbf{u}$, it is now obvious that the unit quaternion can be used for describing a rotation in R^3 as stated at the end of section 2.6. Now the most useful property of the quaternion will be stated in the following theorem:

Theorem 2.7.1. *For any unit quaternion $q = q_0 + \boldsymbol{q} = cos\theta + \boldsymbol{u}sin\theta$ and for any vector $\boldsymbol{v} \in R^3$ the result of the operation $q\boldsymbol{v}q^*$ on $\boldsymbol{v}$ may be interpreted geometrically as a rotation of the vector $\boldsymbol{v}$ through an angle 2θ about $\boldsymbol{q}$ as the axis of rotation.*

For a proof of the theorem, see [17].

2.7.3 Useful formulas

If a quaternion is to be used in a Kalman filter as state space vector x in equation 2.7, a few derivations have to be done. Rotating a vector $\mathbf{v}$ using the quaternion q yielding the vector $\mathbf{u}$ gives:

$$\mathbf{u} = q\mathbf{v}q^*. \tag{2.27}$$

By using definition 2.7.1 and 2.7.2 and writing the vector $\mathbf{v}$ as $\mathbf{v} = v_x\mathbf{i} + v_y\mathbf{j} + v_z\mathbf{k}$, equation 2.27 can be rewritten as:

$$\mathbf{u} = q\mathbf{v}q^* = (q_0 + q_1\mathbf{i} + q_2\mathbf{j} + q_3\mathbf{k})(v_x\mathbf{i} + v_y\mathbf{j} + v_z\mathbf{k})(q_0 - q_1\mathbf{i} - q_2\mathbf{j} - q_3\mathbf{k}). \tag{2.28}$$

By using the multiplication rules given in equation 2.23, equation 2.28 can be rewritten as:

$$\mathbf{u} = q\mathbf{v}q^* = M\mathbf{v}, \tag{2.29}$$

where

$$M = \begin{pmatrix} q_0^2 + q_1^2 - q_2^2 + q_3^2 & 2(q_1q_2 + q_0q_3) & 2(q_1q_3 - q_0q_2) \\ 2(q_1q_2 - q_0q_3) & q_0^2 - q_1^2 + q_2^2 - q_3^2 & 2(q_2q_3 + q_0q_1) \\ 2(q_0q_2 + q_1q_3) & 2(q_2q_3 - q_0q_1) & q_0^2 - q_1^2 - q_2^2 + q_3^2 \end{pmatrix}. \tag{2.30}$$

Since M is the *rotation matrix* or *Direction cosine matrix*, transforming $\mathbf{u}$ to $\mathbf{v}$, a relationship between a quaternion q and a *zyx* Euler sequence has been found. That is, M in equation 2.30 is element wise equal to M_b^l in equation 2.18, given that they represent the

same rotation. This can be used in order to express a rotation known by a quaternion in a zyx Euler rotation sequence. Using elements from equation 2.30 in equation 2.20, we get:

$$\psi = atan2(2(q_1q_2 + q_0q_3), q_0^2 + q_1^2 - q_2^2 + q_3^2) \tag{2.31a}$$
$$\theta = asin(2(q_1q_3 - q_0q_2)) \tag{2.31b}$$
$$\phi = atan2(2(q_2q_3 + q_0q_1), q_0^2 - q_1^2 - q_2^2 + q_3^2). \tag{2.31c}$$

If equation 2.30 is to be used for calculating the function h in equation 2.7b, the Jacobian in equation 2.11 must be calculated:

$$\frac{\partial}{\partial q_j} q v_i q^* = \begin{pmatrix} (q_0, q_3, -q_2)\mathbf{v} & (q_1, q_2, q_3)\mathbf{v} & (-q_2, q_1, -q_0)\mathbf{v} & (-q_3, q_0, q_1)\mathbf{v} \\ (-q_3, q_2, q_3)\mathbf{v} & (q_2, -q_1, q_0)\mathbf{v} & (q_1, q_2, q_3)\mathbf{v} & (-q_0, -q_3, q_2)\mathbf{v} \\ (q_2, -q_1, q_0)\mathbf{v} & (q_3, -q_0, -q_1)\mathbf{v} & (q_0, q_3, -q_2)\mathbf{v} & (q_1, q_2, q_3)\mathbf{v} \end{pmatrix}. \tag{2.32}$$

Each element in equation 2.32, such as $(q_0, q_3, -q_2)\mathbf{v}$, is the scalar product between two 3-dimensional vectors, such that the right hand side of equation 2.32 is a 3 by 4 matrix. The function f in equation 2.7a needs to be calculated, that is, the derivative of q. Two quaternions of unit length, q_a and q_b both representing a rotation can be related by a third unit quaternion q_c representing the rotation between them as:

$$q_a = q_b q_c. \tag{2.33}$$

Now, let $q(t)$ be a unit quaternion representing a rotation at time t and let $q(t + \Delta t)$ be the same quaternion at time $t + \Delta t$ subject to some rotation Δr during Δt

$$q(t + \Delta t) = q(t)\Delta r(t) = q(t)[cos(\frac{\theta}{2}) + \mathbf{v}(t)sin(\frac{\theta}{2})] \tag{2.34}$$

where Δr represents the rotation of angle θ around the axis given by the vector $\mathbf{v}(t)$. Now assuming small Δt and thus small θ gives the following approximation:

$$q(t + \Delta t) = q(t)[1 + (\frac{\theta}{2})\mathbf{v}(t)]. \tag{2.35}$$

The definition of the derivative gives:

$$\frac{d}{dt}q = \lim_{\Delta t \to 0} \frac{q(t + \Delta t) - q(t)}{\Delta t} = \lim_{\Delta t \to 0} \frac{q(t)\mathbf{v}(t)(\frac{\theta}{2})}{\Delta t} = \frac{1}{2}q(t)\bar{\omega}, \tag{2.36}$$

since

$$\lim_{\Delta t \to 0} \frac{\mathbf{v}(t)(\theta)}{\Delta t} = \bar{\omega} \tag{2.37}$$

is a vector representing the angular velocity of the rotation according to the quaternion Δr during the time Δt. Evaluation of $q(t)\bar{\omega}$ term by term gives the derivative of q in matrix form:

$$\frac{d}{dt}q = \frac{1}{2}\begin{pmatrix} 0 & -\omega_x & -\omega_y & -\omega_z \\ \omega_x & 0 & \omega_z & -\omega_y \\ \omega_y & -\omega_z & 0 & \omega_x \\ \omega_z & \omega_y & -\omega_x & 0 \end{pmatrix} q \tag{2.38}$$

where ω_x, ω_y and ω_z are the angular velocities around the axes x, y and z respectively.

2.8 Calibration

The sensors have different possible error sources and the mathematical theory behind their calibration is different. The accelerometer calibration is discussed first followed by the gyroscope calibration and these two are simpler than the calibration of the magnetometer, which is presented last.

2.8.1 Accelerometer calibration

The accelerometers can be calibrated using the fact that the earth gravity is known to both strength and direction. Possible errors include bias, scale factors and axes misalignment. As stated in [4], the relationship between the acceleration applied in the platform frame, a_p, and the acceleration measured in the sensor frame, a_a, can be expressed as:

$$a_a = K_a T_a^p a_p + b_a + v_a \tag{2.39}$$

where K_a is diagonal matrix with scaling coefficients, T_a is a skew matrix compensating for the axes in the sensor not being orthogonal, b_a is a constant bias term and v_a measurement noise. Calculating the misalignment of the sensor axes with high confidence is out of the scope for this thesis and T_a is therefore set to be the identity matrix. If the noise term which is not observable is ignored, the relation reduces to

$$a_a = K_a a_p + b_a \tag{2.40}$$

which has three unknown elements in each of K_a and b_a. If the IMU is placed on each of its six sides, the vertical axis will measure the gravity as a_p, giving a total of six equations and thus K_a and b_a can be solved for uniquely.

2.8.2 Gyroscope calibration

If the gyroscope axes are assumed to be orthogonal and perfectly aligned as in the previous section, the relationship between the angular velocity in the platform frame ω_p and the measurements by the sensor axes ω_g can be expressed as

$$\omega_g = K_g \omega_p + b_g \tag{2.41}$$

where K_g is the scale matrix and b_g the bias or drift. The scale elements in K_g may actually depend on the value of ω and the drift term b_g is often temperature dependent. Taking these facts into account would highly increase the complexity of the calibration procedure and are therefore ignored in this thesis. The drift term b_g can be estimated by simply placing the IMU at rest and taking the mean of the measurements. The scale factor is on the other hand more complicated than for the accelerometer. There is no natural quantity to measure such as the earth gravity for the accelerometer. Instead the sensor has to be subject to some rotational movement. The IMU was attached to a simple office chair for the rotation around each of the three axes. Since a magnetometer was available in this project, the revolutions were detected by analysing the periodicities in these measurements. By assuming K_g being a diagonal matrix, the elements of it could be estimated by equation 2.41 since the true angular velocity is given by the number of revolutions counted from the magnetometer data and the elapsed time.

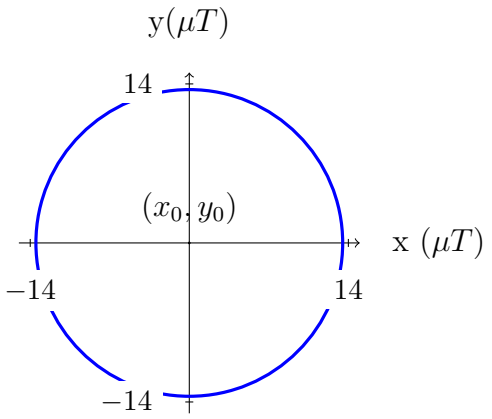

Figure 2.2: The result of rotating the IMU 360° and measuring the magnetic field in an undisturbed environment.

2.8.3 Magnetometer calibration

As stated in [1], disturbances on the magnetometer readings can be put into the categories hard iron, soft iron, non-orthogonalities of the sensors, scaling bias, wideband noise, alignment with the body frame and other effects. The distortions considered in this report will be hard iron, soft iron, Non-orthogonalities of the sensors, scaling and bias.
Hard iron: These disturbances are caused by the presence of ferromagnetic elements and are constant in the body reference frame. Hard iron effects can be thought of as different offsets on the axis of the magnetometer.
Soft Iron: Are not caused directly by a magnetic field. Instead ferromagnetic materials on the same platform as the sensors interact with an outer magnetic field, for instance the earth magnetic field, and alter this. The ferromagnetic material can distort the magnetic field with different strength depending on the orientation of the material relative to the magnetic field.
Non-orthoganities: If the sensor axes are not mounted orthogonal to each other in the IMU, they will partly measure the same component of the magnetic field. At the extreme, all sensor axes might be in the same orientation and will thereby measure the exact same component of the magnetic field.
Scaling: There can be multiplicative errors such that the sensor for instance measures 10% more than the actual value. This error can also be different for the different axes.
Bias: Bias errors will work additively and might add or subtract different constant values to the axes.

Hard iron and soft iron can be explained visually by an example. Let's start by assuming that the horizontal component of the earth magnetic field is being measured using a sensor with two orthoges, call them x and y. Let the strength of the magnetic field be 14 micro Tesla (μT) in a direction straight north. If the sensor axes are kept in a horizontal position and rotated 360° around the z-axis, the measured strength of the magnetic field should always be the same. When facing north, the x-axis will measure $14\mu T$ and the y-axis $0\mu T$ and when facing east, the x-axis will measure $0\mu T$ and the y-axis $-14\mu T$. Completing the 360° and plotting the result as measurement from the x- and y-axis parametrized by the angle, the result should be a circle as shown in figure 2.2.

Now, because of soft iron disturbances, the measured strength of the magnetic field will

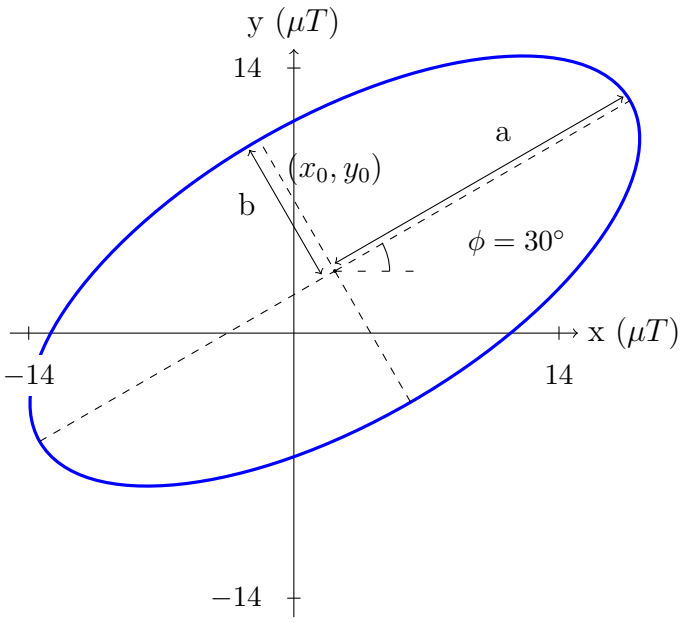

Figure 2.3: The result of rotating the IMU 360° and measuring the magnetic field in the presence of both hard and soft iron disturbances.

depend on the direction of the sensor axes and the result will be that the circle in the plot above turns into an ellipse. The soft iron effect does not necessarily coincide with the sensor axes but might have its maximum effect at some angle ϕ between the x- and y-axis. Because of hard iron effects, there might be an offset in the measurements. For instance there might be some electronic circuit attached to the same frame as the sensors, adding a bias x_0 to the x-axis and y_0 to the y-axis. The effect on the plot will be a shift of the ellipse (or circle if no soft iron effect) by the corresponding bias x_0 and y_0. The result can be seen in figure 2.3 with soft iron disturbances with maximum effect at $\phi = 30°$ and with hard iron disturbances with an offset of x_0 and y_0 on the x- and y-axis respectively. The transformation from earth magnetic field to magnetometer measurements can be expressed mathematically by linear algebra. Following the notation in [1], the measured magnetic field in the sensor frame will be given by:

$$h_r = S_M C_{NO}(C_{SI} R_B^E h_E + b_{HI}) + b_M, \tag{2.42}$$

where h_r is the measured magnetic field in the sensor frame, S_M is a diagonal scaling matrix, C_{NO} comes from the non-orthogonalities of the sensor axis, C_{SI} is the soft iron transformation matrix, R_B^E is the earth to platform transformation matrix, h_E is the earth magnetic field, b_{HI} is the hard iron effect and b_M is the factory offset. Rewriting (2.42) gives:

$$h_r = S_M C_{NO}(C_{SI} R_B^E h_E + b_{HI}) + b_M = S_M C_{NO} C_{SI} R_B^E h_E + S_M C_{NO} b_{HI} + b_M. \tag{2.43}$$

The sensor reading can be written as one part depending on the earth magnetic field and one part being a constant offset. Replacing $S_M C_{NO} C_{SI}$ by M and $S_M C_{NO} b_{HI} + b_M$ by b gives:

$$h_r = M R_B^E h_E + b = M h_B + b \tag{2.44}$$

where h_B is the earth magnetic field in the body frame. For this application, there is no way to distinguish between the hard iron distortion and the factory bias, so their combined effect, b, will be of interest. To reduce the number of non-zero elements in C_{NO} as in [4], the platform coordinate z-axis is defined to coincide with the magnetometer z sensitivity axis, and the y magnetometer axis is defined to lie in the plane spanned by the magnetometer z- and y-axis. As stated in [2] the soft iron distortions can be split into a combination of scale errors and misalignment and can therefore be written as an over triangular matrix, with the same convention as for C_{NO}. Replacing h_B by $\hat{m}$ to denote the measured magnetic field and h_B by m to denote the magnetic field in the body frame gives:

$$\begin{pmatrix} \hat{m}_x \\ \hat{m}_y \\ \hat{m}_z \end{pmatrix} = \begin{pmatrix} \beta_{11} & \beta_{12} & \beta_{13} \\ 0 & \beta_{22} & \beta_{23} \\ 0 & 0 & \beta_{33} \end{pmatrix} \begin{pmatrix} m_x \\ m_y \\ m_z \end{pmatrix} + \begin{pmatrix} b_x \\ b_y \\ b_z \end{pmatrix} \tag{2.45}$$

or equivalently :

$$\begin{pmatrix} m_x \\ m_y \\ m_z \end{pmatrix} = \begin{pmatrix} \alpha_{11} & \alpha_{12} & \alpha_{13} \\ 0 & \alpha_{22} & \alpha_{23} \\ 0 & 0 & \alpha_{33} \end{pmatrix} \begin{pmatrix} \hat{m}_x - b_x \\ \hat{m}_y - b_y \\ \hat{m}_z - b_z \end{pmatrix}. \tag{2.46}$$

The aim of the calibration procedure will be to find the 9 unknown parameters in (2.46). Putting the IMU on each of its six sides and comparing the measurement from the axis pointing upwards with the vertical component of the earth magnetic field gives six equation. In order to compare the component of the magnetic field lying in the horizontal plane pointing north with one of the axis, the direction toward north must be known. Since this is the aim of the project, this direction must be considered unknown and cannot be used for comparing directly with the sensor measurements. The horizontal norm however will be known and can be be compared with the norm of the two axes of the magnetometer lying in the horizontal plane. When, for instance, putting the IMU in such way that the y-axis points up, equation 2.46 gives:

$$\alpha_{22}(\hat{m}_y - b_y) + \alpha_{23}(\hat{m}_z - b_z) - m_{up} = 0 \tag{2.47a}$$

and

$$\begin{aligned} &(\alpha_{11}(\hat{m}_x - b_x) + \alpha_{12}(\hat{m}_y - b_y) + \alpha_{13}(\hat{m}_z - b_z))^2 \\ &\qquad +(\alpha_{33}(\hat{m}_z - b_z))^2 - m_{hor}^2 = \\ &(\alpha_{11}(\hat{m}_x - b_x) + \alpha_{12}(\hat{m}_y - b_y) + \alpha_{13}(\hat{m}_z - b_z))^2 \\ &\qquad +(\alpha_{33}(\hat{m}_z - b_z))^2 - (m_x^2 + m_z^2) = 0. \end{aligned} \tag{2.47b}$$

Where (2.47a) comes from comparing the measurement in y-direction with the vertical component of the magnetic field and (2.47b) comes from comparing the norm of the measurements in the x and z direction with the horizontal component of the earth magnetic field. One additional equation identical to (2.47a) will be received from the measurement when putting the y-axis pointing down. This will however not give any additional information concerning the horizontal plane, since the same axes still measure the same field component. Note that the IMU must be put on a horizontal surface in order to set the vertical component of the earth magnetic field equal to the vertical body axis. The three axes give three equations each, giving nine equations in total to solve for nine unknown. Since the system of equations in non-linear, it has to be solved numerically. A simple way to solve this is to use Newton's method [5] given in the pseudo code in algorithm 1.

Data: Magnetometer measurements from 6 directions, initial guess
Result: skew matrix and bias
Initialization;
while $|F| >$ *some tolerance* **do**
  compute F=$F(x)$
  compute J=$J(x)$
  dx=$-JF^{-1}$
  $x = x + dx$
end

Algorithm 1: Newton's method

x is a vector containing the 9 unknown mentioned above, $F(x)$ is the value of the nine equations mentioned above and J is the 9 by 9 Jacobian computed as

$$J_{i,j}(x) = \frac{\partial}{\partial x_j} F_i. \tag{2.48}$$

Chapter 3

Attitude system

The purpose of the attitude system is to keep track of what rotation of the sensor data is needed in order to calculate the measured heading and the heading velocity from the magnetometer and gyroscope respectively. Some problems occur since the acceleration of the body and the Earth's gravity vector can not be distinguished from each other through the accelerometer measurements. The first section presents how the attitude system can adapt the utility of the different sensors according to this fact. The attitude system represented by a quaternion is presented in the next section followed by a redefinition of heading due to extreme positions in the last section.

3.1 Accelerometer disturbances

The attitude system will be updated by measuring the earth gravity vector by the accelerometer. However, when the person wearing the IMU performs activities such as walking and running, these will have large impact on the accelerometer. For instance when running, the accelerometer could measure zero acceleration in all dimension when both feet are in the air, while the acceleration at the moment when a foot touches the ground can be much greater than the norm of earth gravity vector $|g|$. A quaternion will be used for representation of the attitude. The quaternion will be the state space variable in a state space model that will utilize an EKF for a better estimation of the attitude as discussed in section 2.2. The matrix R, that is, the covariance of the noise variable v_k in equation 2.2b, represents the amount of noise in the measurement of the system. Therefore, it seems logical that the matrix R should have large elements when the disturbances on the accelerometer are great and have smaller elements otherwise. From here on, R will be assumed to be a matrix with all diagonal elements equal to r and all non-diagonal elements equal to zero. The benefit of this adjustment would be that errors in the attitude due to gyroscope drift is avoided when the accelerometer can be trusted and that errors from the accelerometers are avoided when this sensor is noisy due to rapid movement. The square of the deviation of the norm of the accelerometer measurement vector $|a_k|$ from $|g|$, where k represents the time instance, seems like a good measure on how disturbed it is. Let $\Delta_k = (|a_k| - |g|)^2$ be this deviation. Adjusting r with respect to the instantaneous value of Δ_k will not be a good idea, since Δ_k will oscillate and there will be situations even when running when $\Delta_k = 0$, fooling the Kalman filter to believe the accelerometer to be more reliable than it is. Two possible approaches for a better measure are:

- The variance $V = \frac{1}{N}\sum_{k=1}^{N}(|a_k| - |g|)^2$

- A low pass filtered signal $d[z] = F[z]\Delta_k[z]$ for some filter with transfer function F(z).

The first approach would need either to store N values or only update every N sample. It would also be relatively noisy compared to the second solution since N in most cases would not correspond to exactly one period of the movement. The second solution does not need much storage and noise can be suppressed. A time delay will however be introduced and the implementation will be a trade off between time delay and noise suppression. A first order low pass filter is chosen according to equation 2.13, resulting in:

$$d_k = \alpha d_{k-1} + (1-\alpha)(|a_k| - |g|)^2. \tag{3.1}$$

The filter constant α is set depending on what time constant is desired. Since the time between two steps is less than 1 second for most of the time during walking and running, this seems sufficient in order not to underestimate the noise. Using equation 2.17 gives $\alpha = 0.9918$ for $\tau = 1s$ and for the sample time $T_s = 8.3ms$ used in this project.

Now, the variable d_k is a measure on how disturbed the accelerometer is and the value of the variable r, which sets the values of the noise covariance matrix R in the EKF, should be changed accordingly. A simple and intuitive approach would be to choose the value of r from a set of predefined values known beforehand to be good for the specific amount of noise. Since the value of d_k has typical values depending on if the person is standing still, walking or running, a good idea might be to choose from three different values on r. When the value of d_k increases above or decreases below some predefined threshold, the value of r should be changed accordingly. The thresholds on the variable d_k for when to increase or decrease r can be derived empirically and should be chosen with some hysteresis in order to avoid too much fluctuations in the value of r. This means that the threshold on d_k for increasing r from some value a to some value b is higher than that to decrease r from b to a. A problem that can occur when the person goes from walking to running and r is increased, is caused by the fact that the EKF cannot distinguish between an external acceleration and the Earth's gravity vector. Increasing the speed will introduce an horizontal component in the accelerometer measurement which the EKF will interpret as if the body was tilted in that direction. This introduces an error and when r thereafter is increased to trust the gyroscope more, this error will last longer than if r was not changed. A solution to this is to constantly calculate the value of two additional quaternions in the background and only update them based on the gyroscope. The two quaternions in the background should be reset unsynchronized every say 10 seconds, since they would diverge from the true value otherwise. When r is increased, the oldest of these quaternion should replace the state quaternion and thereby avoiding the external acceleration.

3.2 Update equations

A unit quaternion $q_k = (q_{k,0}, q_{k,1}, q_{k,2}, q_{k,3})^T$ is used as a 4-dimensional state space variable representing the attitude system at time instance k. The quaternion thus corresponds to the variable x in equation 2.7. The measurement from the gyroscope gives the derivative of the quaternion and therefore, in the discrete state space, gives the difference from one sample to the other. This corresponds to the prediction step in equation 2.8. The accelerometer data is used for observing the absolute attitude of the system, corresponding to the update step in equation 2.9. This is done by comparing the known gravity vector with the measured acceleration vector. Before these two can be compared directly, one of them has to be rotated such that they are both represented in the same coordinate system.

Since the rotation matrix from earth gravity vector g to the accelerometer measurements a_k is non-linear in terms of q, an EKF is used. It is worth to note, that in terms of Euler angles, the pitch and roll angles can be observed through a, while the heading can not. Even if the quaternion is initialized correctly and the true heading can be derived from it in the beginning, this information will be lost quickly due to noise in gyroscope measurements, with no possibility of correction from the accelerometer. Because of this, the magnetometer is essential to the heading estimation.

Before the first measurements from the sensors are being used, the quaternion and the state covariance matrix need to be initialized. The quaternion will be initialized as $q_0 = (1, 0, 0, 0)^T$ corresponding to no rotation and the covariance matrix will be initialized to $P = 1000I$, where I is a 4 by 4 unit matrix. The value of q_0 is chosen since it is most likely that the person is starting in a standing position and the covariance matrix is chosen with great elements in order to make q quickly converge to the true value. Now for each sample from the sensors, the following calculations will be performed:

The predictions $\hat{q}_{k|k-1}$ and $P_{k|k-1}$ are calculated according to equation 2.4 as

$$\hat{q}_{k|k-1} = F_k \hat{q}_{k-1|k-1} = \frac{T_s}{2} \begin{pmatrix} \frac{2}{T_s} & -\omega_x & -\omega_y & -\omega_z \\ \omega_x & \frac{2}{T_s} & \omega_z & -\omega_y \\ \omega_y & -\omega_z & \frac{2}{T_s} & \omega_x \\ \omega_z & \omega_y & -\omega_x & \frac{2}{T_s} \end{pmatrix} \hat{q}_{k-1|k-1} \tag{3.2}$$

where F_k is given by equation 2.38, T_s is the sample time and

$$P_{k|k-1} = F_k P_{k-1|k-1} F_k^T + Q_k. \tag{3.3}$$

The assumption that the angular velocity is constant during T_s is made here. This is not completely true, but a good approximation since the used sample time in the project, $T_s = 8.3ms$ is very small in relation to the movements of a human body.

The low-pass filtered value of the disturbances on the accelerometer, d_k is calculated according to equation 3.1 with $\alpha = 0.9918$ corresponding to a time constant of $\tau = 1s$ given the sample frequency $121Hz$ by equation 2.17 as:

$$d_k = 0.9918 d_{k-1} + 0.0082(|a_k| - 9.81)^2. \tag{3.4}$$

The value of d_k will set the values in the matrix R_k as discussed in section 3.1. For a person, three behaviors that have very characteristic values on d_k are standing, walking and running. Therefore R_k was chosen from a set of three possible values each representing an interval on d_k. To avoid R_k from fluctuating between two values when d_k is on the limit between two intervals, a hysteresis is used such that the values for increasing and decreasing R is not he same. In order to perform the update step in equation 2.5, H_k needs to be calculated according to equation 2.32. This is because what is observed through the accelerometer is modeled to be the earth gravity vector $\mathbf{g}$ measured in the body frame, $\mathbf{g}^b = q\mathbf{g}q^*$ according to 2.27. Taking the Hessian with respect to q gives :

$$H_k = \begin{pmatrix} (q_{k,0}, q_{k,3}, -q_{k,2})\mathbf{g} & (q_{k,1}, q_{k,2}, q_{k,3})\mathbf{g} & (-q_{k,2}, q_{k,1}, -q_{k,0})\mathbf{g} & (-q_{k,3}, q_{k,0}, q_{k,1})\mathbf{g} \\ (-q_{k,3}, q_{k,2}, q_{k,3})\mathbf{g} & (q_{k,2}, -q_{k,1}, q_{k,0})\mathbf{g} & (q_{k,1}, q_{k,2}, q_{k,3})\mathbf{g} & (-q_{k,0}, -q_{k,3}, q_{k,2})\mathbf{g} \\ (q_{k,2}, -q_{k,1}, q_{k,0})\mathbf{g} & (q_{k,3}, -q_{k,0}, -q_{k,1})\mathbf{g} & (q_{k,0}, q_{k,3}, -q_{k,2})\mathbf{g} & (q_{k,1}, q_{k,2}, q_{k,3})\mathbf{g} \end{pmatrix}, \tag{3.5}$$

which is a 3 by 4 matrix where each element is calculated from a scalar product. Now the Kalman gain in equation 2.6 can be calculated:

$$K_k = P_{k|k-1}H_k^T(H_kP_{k|k-1}H_k^T + R_k)^{-1}, \tag{3.6}$$

and the updated q and P are given by equation 2.5

$$\hat{q}_{k|k} = \hat{q}_{k|k-1} + K_k(a_k - H_k\hat{q}_{k|k-1}) \tag{3.7a}$$
$$P_{k|k} = (I - K_kH_k)P_{k|k-1}. \tag{3.7b}$$

For the quaternion to represent a spatial rotation, it is crucial that it is in fact a unit quaternion as defined in definition 2.7.2. Since the measurements from the gyroscope contain noise, the norm of the quaternion might start to differ from 1 and therefore it needs to be normalized. This is done in each iteration, such that the final output in each iteration is:

$$\hat{q}_{k|k} \leftarrow \frac{\hat{q}_{k|k}}{\sqrt{q_{k,0}^2 + q_{k,1}^2 + q_{k,2}^2 + q_{k,3}^2}} \tag{3.8}$$

where $q_{k,0}, ...q_{k,3}$ represents the elements of $\hat{q}_{k|k}$. The procedure can be summarized in algorithm 2.

Initialization: $q_0 = (1, 0, 0, 0)^T$, $P_0 = 1000I$;
Data: ω_k, a_k, $\hat{q}_{k-1|k-1}$, P_{k-1}
Result: $\hat{q}_{k|k}$, P_k
for *each sample* k **do**
  Use $\hat{q}_{k-1|k-1}$ to predict $\hat{q}_{k|k-1}$ using equation 3.2
  Compute accelerometer disturbance d from a_k and set R_k using equation 3.4
  Calculate H_k using equation 3.5
  Calculate K_k using equation 3.6
  Update $\hat{q}_{k|k-1}$ to get $\hat{q}_{k|k}$ using equation 3.7a
  Update $P_{k|k-1}$ to get $P_{k|k}$ using equation 3.7b
  Normalize $\hat{q}_{k|k}$ using equation 3.8
end

Algorithm 2: Quaternion update

3.3 Redefining heading

In situations when the pitch angle is equal to $\pm 90°$, the heading is not defined. When the pitch is close to these values, the heading is defined but can be unstable. For instance, a small rotation in pitch angle from $-89°$ to $-91°$ results in a jump in heading angle with $180°$. For the roll angle, this problem does not occur in the same way; since a rotation performed purely in the roll angle is a rotation around the x-axis, it cannot affect the heading. However, for this specific application, large roll angle may still make redefinition of the heading useful. Imagine a situation when the roll angle is $90°$, corresponding to the person lying on the side. It seems unlikely that the person will be able to simple rotate back the very same way, i.e. somehow manage to rise from lying on the side to standing by only rotating around the x-axis of the body. In most situation in reality, the person would first rotate to a face-down position and then rise. It seems plausible that in situations when either the roll or the pitch angle is close to $\pm 90°$, the heading can be redefined to mean *the angle between the projection of the head to the horizontal plane and*

north. Actually, this is the same definition as for the heading in definition 2.5.1, except for now projecting the negative z-axis instead of the x-axis:

Definition 3.3.1. *In situations when the original definition of the heading is not appropriate, the heading ψ_{rd}, is the angle between the projection of the negative z-axis to the horizontal plane and geographic north, such that $\psi_{rd} \in (-180°, 180°]$. The angle is positive if the projection of the negative z-axis is pointing to the right of north and negative if it points to the left of north.*

The redefined heading will still be given by the same quaternion representing the attitude of the person. The heading can be computed with the exact formulas as before, with the modification that the new x-axis coincides with the old z-axis, the new and old y-axis being the same and the new z-axis completing the right hand rule. This corresponds to first rotating the system 90 degrees around the y-axis. Thus qvq^* is replaced by

$$qq_y v q_y^* q^* = q_{tot} v q_{tot}^* \tag{3.9}$$

where

$$q_y = (cos(\tfrac{\frac{\pi}{2}}{2}), 0, sin(\tfrac{\frac{\pi}{2}}{2})cos(0), 0)^T = \frac{1}{\sqrt{2}}(1, 0, 1, 0)^T, \tag{3.10}$$

$$q_{tot} = qq_y = \frac{1}{\sqrt{2}}(q_0 - q_2, q_1 - q_3, q_2 + q_0, q_3 + q_1)^T. \tag{3.11}$$

Example 3.3.1 shows one benefit with the redefined heading:

Example 3.3.1. *Starting from a standing position facing north, the person is laying down and starting crawling down a gentle slope. Let this rotation be $-\frac{1.1\pi}{2}$ around the y-axis. This rotation corresponds to a quaternion $q = (cos(-\frac{1.1\pi/2}{2}), 0, sin(-\frac{1.1\pi/2}{2}), 0)^T \approx (0.649, 0, -0.760, 0)^T$. To redefine the heading we would instead use q_{tot} in equation 3.11, $q_{tot} = (0.997, 0, -0.078, 0)^T$ Using the different definitions of the heading, we achieve different results: $\psi = 180°$ and $\psi_{rd} = 0°$. When considering the situation of the person crawling toward north, it seems however to make more sense with the heading being* 0 *rather than* 180*.*

When to use the alternative definition of the heading is still to be decided. As mentioned before, doing so is desirable in situations when either pitch angle or roll angle is close to $\pm 90°$. In fact, any combination in which these angles together causes the person to be in a somewhat horizontal position, are subject to the redefinition. A simple way to evaluate to which extent the person is lying down is to calculate

$$h(q) = (-\mathbf{z})^T q(\text{-}\mathbf{z})q^* \tag{3.12}$$

where -**z** is the unit vector $(0, 0, -1)^T$ and q is the quaternion representing the attitude. This is the scalar product between the negative z-axis and the negative z-axis rotated according to the quaternion. In this application, it corresponds to the height of the head above ground for a person of unit length rotated with respect to the quaternion. For instance, $h(q) = 1$ corresponds to the person standing up, $h(q) = 0$ corresponds to the person lying flat down and $h(q) = -1$ corresponds to the person standing upside down. Now since $q\mathbf{v}q^*$ is given for any vector $\mathbf{v}$ by equation 2.30, $h(q)$ is in fact given by element (3,3) in the DCM with opposite sign:

$$h(q) = -DCM(q)_{(3,3)} = -q_0^2 + q_1^2 + q_2^2 - q_3^2. \tag{3.13}$$

Finally, a numerical limit should be set for the value of $h(q)$ defining when the redefinition should be done. This limit can be set with a hysteresis in order to avoid quickly repeated changes between the two definitions.

Chapter 4

Fusion of measured heading and heading velocity

4.1 Problem statement

By using the pitch and roll angle from the attitude system, the measurements from the magnetometer and from the gyroscope in body coordinates can be transformed into their horizontal counterparts. That is, a coordinate system with neither pitch nor roll but with the same heading as given by the body coordinates. The magnetometer data will then give the measured heading and the gyroscope data will give the velocity of the heading. The simplest possible state space model would be:

$$\psi^m_{k+1} = \psi^m_k + T_s\dot{\psi}^g_k + w_k \tag{4.1a}$$

$$z_k = \psi^{mm}_k + v_k \tag{4.1b}$$

where $\dot{\psi}^g_k$ is the heading velocity measured by the gyroscope, ψ^{mm}_k is the heading measured by the magnetometer and T_s is the sampling time. A natural approach to get a better estimation of the magnetic heading is to use a state observer:

$$\psi^m_{k+1} = \psi^m_k + T_s\dot{\psi}^g_k + K(\psi^{mm}_k - (\psi^m_k + T_s\dot{\psi}^g_k)) = K(\psi^{mm}_k) + (1-K)(\psi^m_k + T_s\dot{\psi}^g_k). \tag{4.2}$$

There is an important difference between the two variables ψ^m and ψ^{mm}, that was stated in section 1.4 : The variable ψ^{mm} is the measured heading by the magnetometer while ψ^m is the filtered version, taking the velocity of the heading measured by the gyroscope into account. Both these variables measures the angle toward the Earth's magnetic north pole and not the geographic one, since the declination is not taken into account.

The main challenge implementing equation 4.2 is to set the value of K. The measurement noise of the gyroscope remains approximately constant over time, since it is not dependent on body movements or environmental circumstances. The magnetometer however, is very sensitive to disturbances in the magnetic field. While the measurements are reliable outdoors in absence of ferromagnetic material, they may be completely useless indoors when other fields than the earth magnetic field are present. One indicator for deciding whether the magnetometer is being disturbed or not is the norm of the magnetometer measurement, or the strength of the measured magnetic field. It varies slightly outside due to ferromagnetic material in the ground but can be modeled to be approximately constant. If the strength deviates from its nominal value, the magnetometer can be considered disturbed.

4.2 Magnetic field strength

The strength of the earth magnetic field in Stockholm, where the experiments in this report were performed is around 52 micro Tesla (μT). When the magnetometer is being disturbed, the strength is changed significantly. A first approach to avoid magnetic disturbances would be to set $K = 0$ in equation 4.2 as soon as the strength deviates from its reference value ($52\mu T$) by more than some limit. The resulting update equation would then be

$$\psi^m_{k+1} = \psi^m_k + T_s\dot{\psi}^g_k \tag{4.3}$$

which is equivalent to integrating the gyroscope measurements. This can be done, depending on the quality of the sensors, for some amount of time before the gyroscope drift and non-linearities has introduced too much error. Since the magnetometer measurements are noisy, some deviation in strength has to be allowed before K can be set to zero. In order to avoid introducing error to the magnetic heading while the magnetometer is beginning to be disturbed but the strength has not yet reached the limit, two alternative heading estimations will be calculated in the background continually. These will only be calculated by integrating the gyroscope measurements and can be reset from the magnetic heading estimation every, say 10 seconds and can replace the disturbed magnetic heading when the limit in strength is passed. They are denoted ψ_{g1} and ψ_{g2} and are updated as:

$$\psi_{g1}(n) = \begin{cases} \psi^m & \text{if } mod(n, N) = 0 \\ \psi_{g1}(n-1) + T_s\dot{\psi}_g & \text{else} \end{cases} \tag{4.4a}$$

$$\psi_{g2}(n) = \begin{cases} \psi^m & \text{if } mod(n + N/2, N) = 0 \\ \psi_{g2}(n-1) + T_s\dot{\psi}_g & \text{else} \end{cases} \tag{4.4b}$$

where ψ^m denotes the final estimation of the magnetic heading from the system, T_s the sample time and $\dot{\psi}_g$ the velocity of the heading from the gyroscope. When navigation is performed indoors, the strength can be decreased to, say $40\mu T$, but still have the correct direction i.e the same direction as it would have had if the building was not there. So in a situation when the person is entering a building the strength of the magnetic field will first decrease below the limit in order to set $K = 0$ and possibly stay there until the person exits the building. This will cause the magnetic heading to diffuse away from its true value unless there is some method to again "trust" the magnetometer, even if the strength of the magnetic field is not correct. Because of this, the instantaneous strength should be compared to a low pass filtered value on the strength, instead of predefining it. According to section 2.3, a first order low pass filter with a constant equal to 0.997 gives a time constant of $\tau \approx 3s$ if $T_s = 8.3ms$. A measure on how much the strength deviates from this is:

$$\Delta m = ||m| - |m_{lp}|| \tag{4.5}$$

where $|m|$ is the instantaneous strength and $|m_{lp}|$ is the low pass filtered norm. This method works well regarding disturbances that causes the strength of the magnetic field to increase or decrease. However, if the the strength of the magnetic field oscillates without changing the direction of the magnetic field vector, this will still be classified as a disturbance. A method for detecting disturbances that are not based on the strength of the magnetic field was developed during the project, but is due to patent matters not covered in this version of the report.

Chapter 5

Magnetic declination

In order to find the magnetic declination, the heading based on the magnetometer measurements was compared to the course calculated by the GPS. The course is the tangent to the path travelled while the heading is related to the coordinate system of the body. If for instance the person is moving backwards, the course and the heading will differ by 180°. If the IMU is not mounted correctly on the person, additional difference between the heading and the course will be introduced. Since step classification is not part of this thesis and since wrongly mounted IMU would be very difficult to differentiate from magnetic declination, test was performed with only straight walk with the IMU correctly mounted. In addition, both the GPS and the sensors were assumed to be undisturbed. For a number N of sequences of straight walk, the magnetic declination $\Delta\psi$ was calculated by:

$$\Delta\psi = \frac{1}{N}\sum_{i=1}^{N}\Delta\psi_i \tag{5.1}$$

where $\Delta\psi_i$ is the declination calculated by walking in the direction i and given by:

$$\Delta\psi_i = \frac{1}{K}\sum_{j=1}^{K}\psi_m(j) - \theta_{GPS}(j) \tag{5.2}$$

where $\psi_m(j)$ is the magnetic heading and $\theta_{GPS}(j)$ the course from the GPS for the j:th sample point out of K.

Chapter 6

Experimental results

6.1 Evaluation of calibration

To see the difference between the calibrated magnetometer data and the uncalibrated one, the IMU was rotated a few times around the x-axis. The raw data can be seen in figure 6.1 and the calibrated data in figure 6.2. If the data would not need to be calibrated, this rotation would yield a circle according to the discussion in section 2.8.3. As can be seen, there is a big offset in the z-direction, which would make the measurements almost useless if not calibrated for. There is also a small difference in scaling between the axes, the horizontal radius is slightly larger. Considering the calibration theory and equation 2.44: $h_r = Mh_B + b$, the hard iron/factory-bias b was often as large as 50% of the measured value for the z-axis. The non-diagonal terms of M was too small to significantly measure with the given equipment and the diagonal terms of M, i.e scaling and soft iron effects, differed up to 20% between the largest and the smallest value.

6.2 Evaluation of attitude system

The redefinition of the heading during extreme attitudes was tested in a typical situation that it was intended for. During simulation outside in a flat environment, a test person walked a few steps, bent down and crawled for about 30 seconds and then got up and took a few steps. The value of $h(q)$ from equation 3.13 was calculated and if $h(q) < 0.6$ the redefinition of the heading was used such that the quaternion representing the attitude was set according to equation 3.11. If then $h(q) > 0.7$, the original definition was again used. The result can be seen in figure 6.3. In black is the original version of the heading and in blue the redefinition, taking the extreme attitude into account. During walking at the beginning and the end, the two headings are identical while they differ during the crawling motion. The advantage with the redefined heading is the fact that it oscillates around the direction of movement while the original definition gives a value hard to interpret in terms of direction.

Next, the methods for changing the covariance matrix R for the accelerometer in the quaternion discussed in section 3.1 were tested. R was always a 3 by 3 diagonal matrix with the same value for all the diagonal elements, denoted r. Primarily, three different values for r were tested for the same data. The data was collected during a sequence of standing, walking, running and standing, all in approximately the same direction. In figure 6.4 when $r = 10^7$, there is no drift during standing still but the amplitude of the oscillations during running is about 50°. In figure 6.5 when $r_=10^8$ the amplitude is smaller

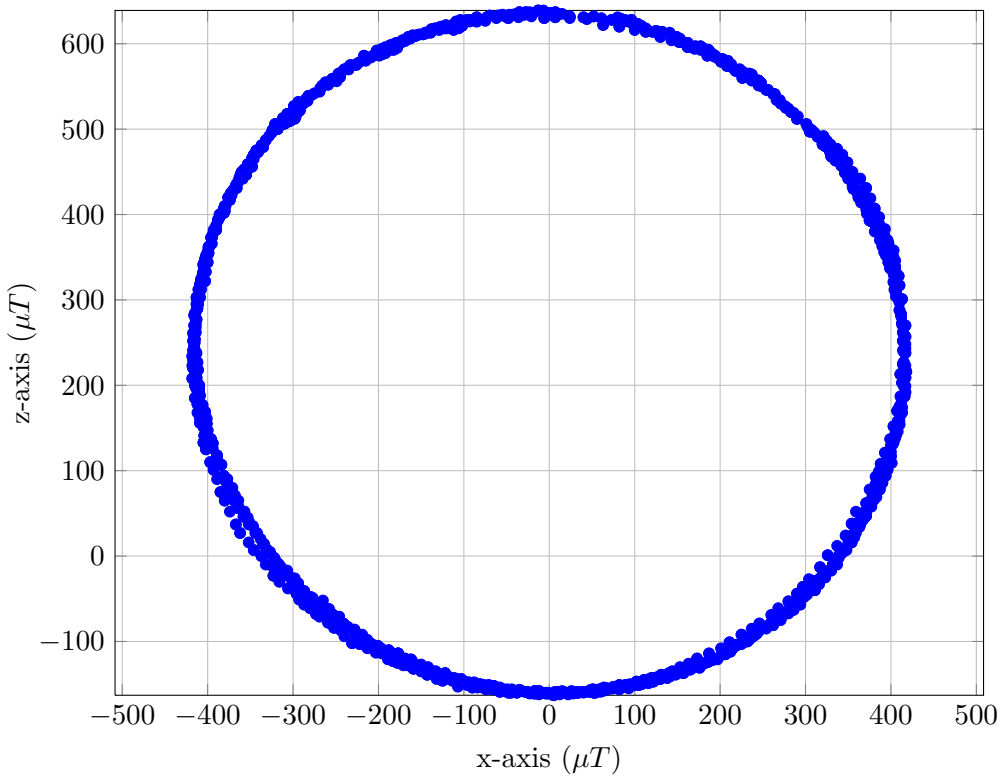

Figure 6.1: Uncalibrated magnetometer data for y-axis and z-axis when rotating the IMU a few laps around the x-axis. A big offset in z-direction can be seen.

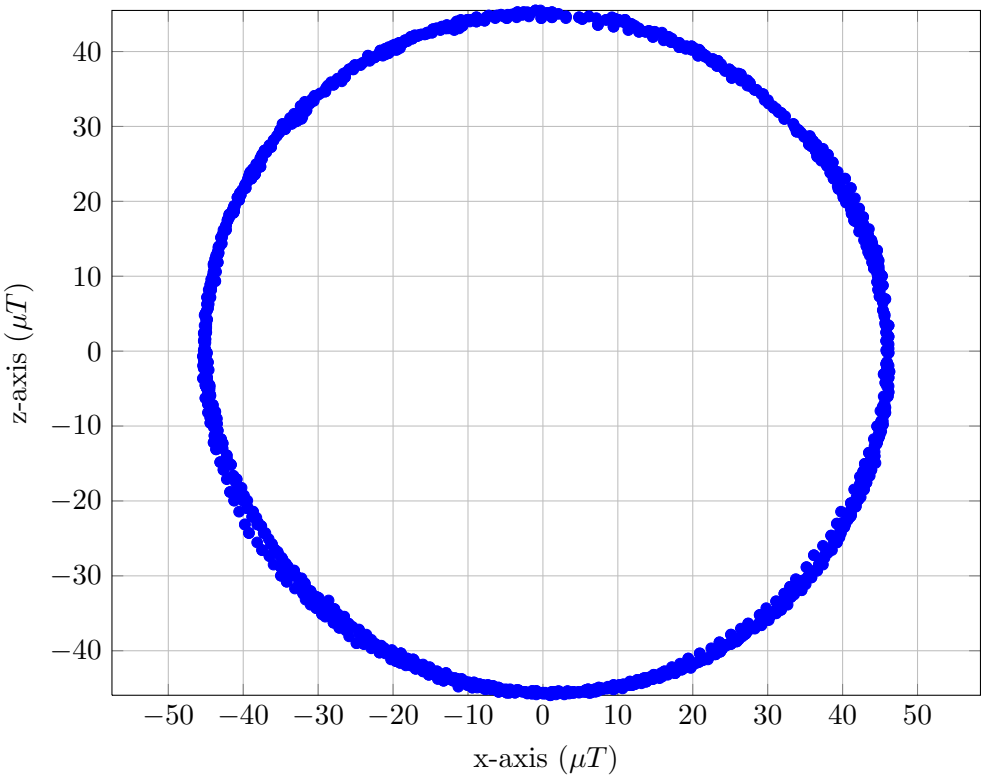

Figure 6.2: Calibrated magnetometer data for y-axis and z-axis when rotating the IMU a few laps around the x-axis. The centre of the circle is now the origin.

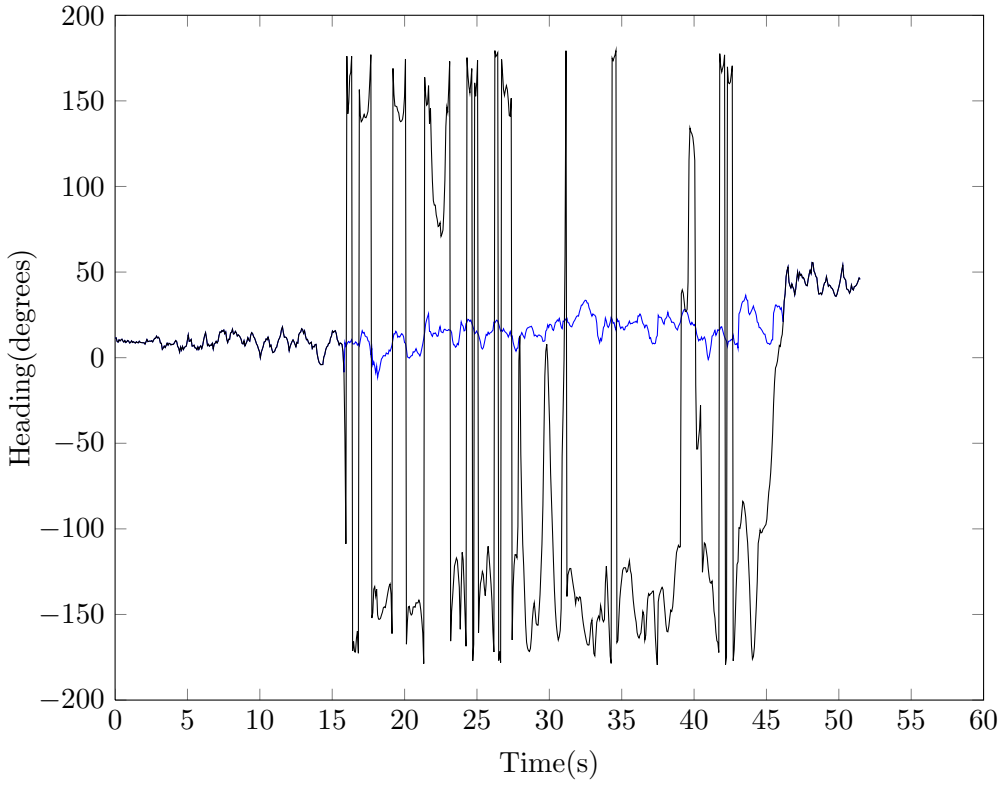

Figure 6.3: Heading calculated from magnetometer data during forward walk and crawling. Using the original definition in black and using the redefinition in blue.

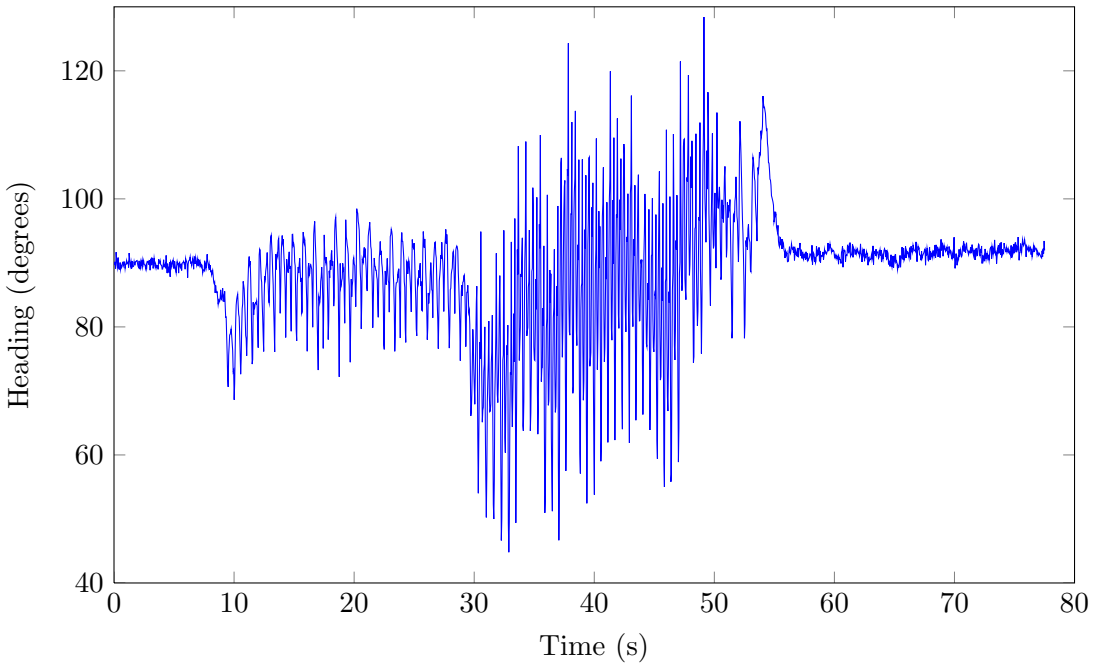

Figure 6.4: Measured heading when using $r = 10^7$ in the EKF for the attitude system.

but an error is introduced during running which gradually fades away at around $t = 55s$ to $t = 70s$. In figure 6.6 when $r = 10^9$, the amplitude of the measured heading during running is smaller than for the previous value of R, but the same bias is introduced near the end. In figure 6.7, R is changed depending on the value of the low pass filtered variance of the accelerometer and the technique of back tracking the attitude to avoid influences from external acceleration is incorporated. The values for r was set to $10^7, 10^8$ and 10^9 and the limits for increasing r based on d_k in equation 3.1 was 2 and 40, and for decreasing it, 1 and 20. As can be seen, the amplitude during running is as low as when $r = 10^9$ while the error when standing at the end is eliminated.

6.3 Magnetic declination

The magnetic declination was estimated during straight walk outdoors in 4 different directions for about 50 seconds each. The experiment can be seen in figure 6.8 where the magnetic heading from the fusion between magnetometer and gyroscope is plotted in black along with the course from the GPS in blue. The mean difference in the 4 directions were: 9.5°, 7.2°, 4.7° and 6.8° degrees by equation 5.2 and the declination was then 7.0° by equation 5.1. The experiment was performed in Stockholm where the declination is 5.15°.

6.4 Accuracy of the magnetometer

Throughout the project, the heading calculated from the magnetometer was from time to time very inaccurate. The magnetometer was suspected to be the cause of these problems, since it was beforehand known to be a cheap sensor. In order to find possible malfunctions in the magnetometer, the IMU was put on the ground untouched for about 5 minutes in an undisturbed environment. The result for the three axes can be seen in figure 6.9.

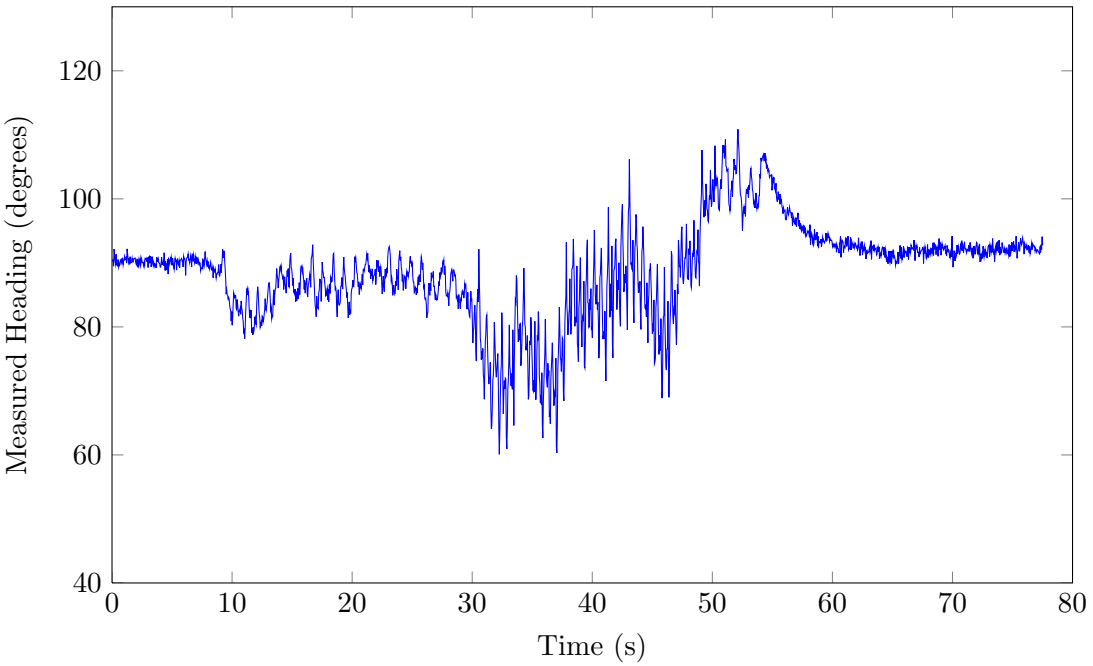

Figure 6.5: Measured heading when using $r = 10^8$ in the EKF for the attitude system.

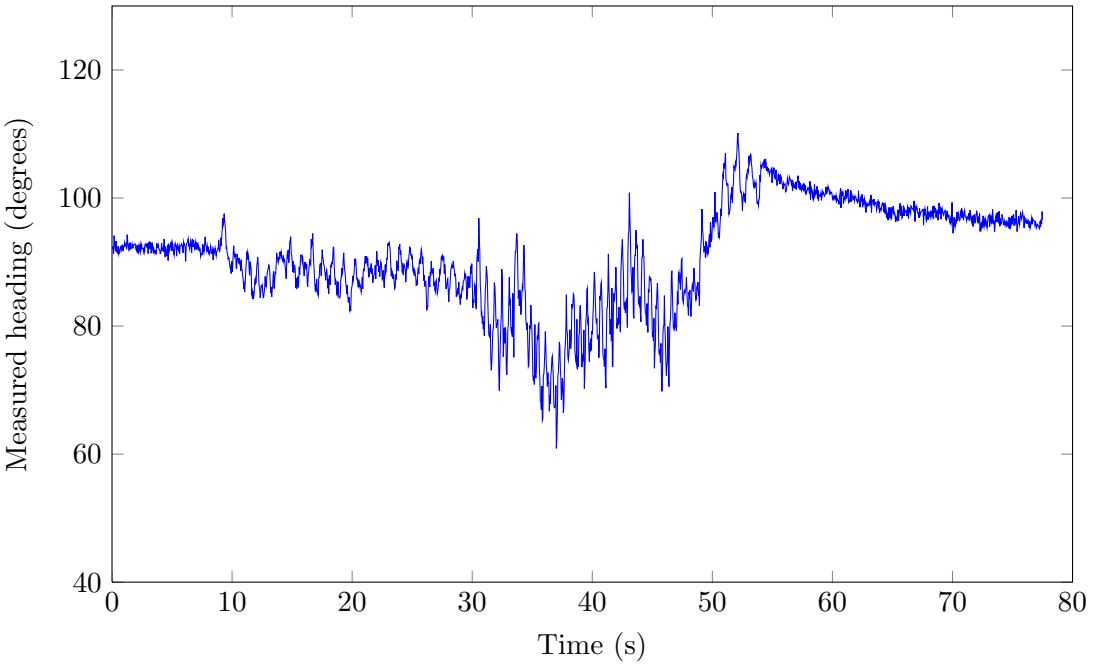

Figure 6.6: Measured heading when using $r = 10^9$ in the EKF for the attitude system.

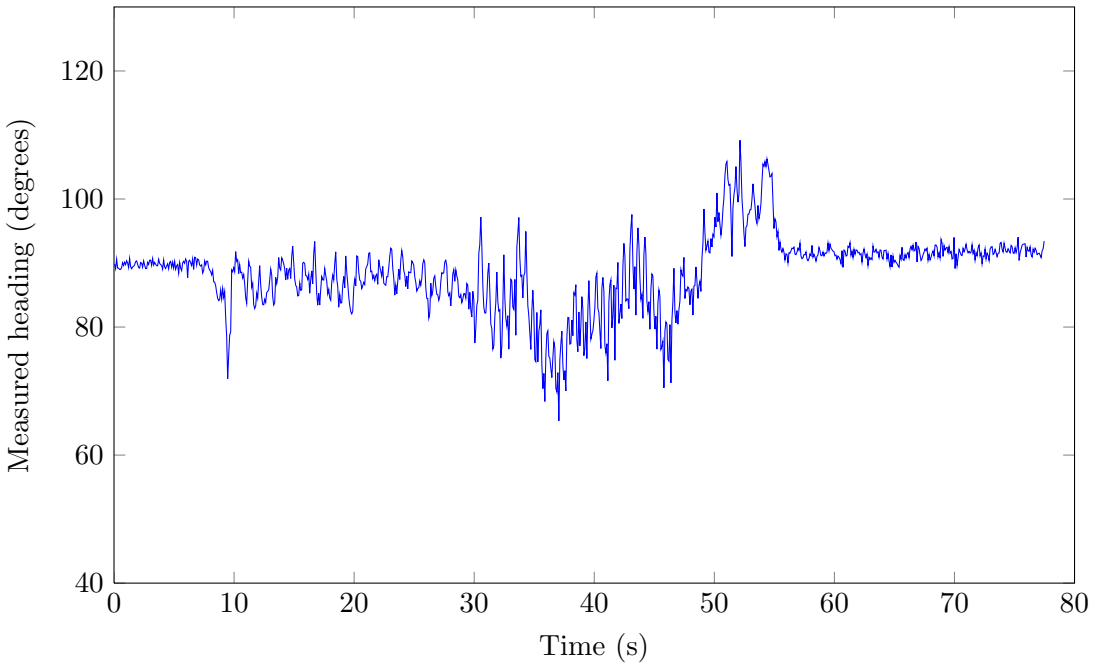

Figure 6.7: Measured heading setting r according to the variance in the accelerometer measurements and back tracking to avoid the influence from external acceleration.

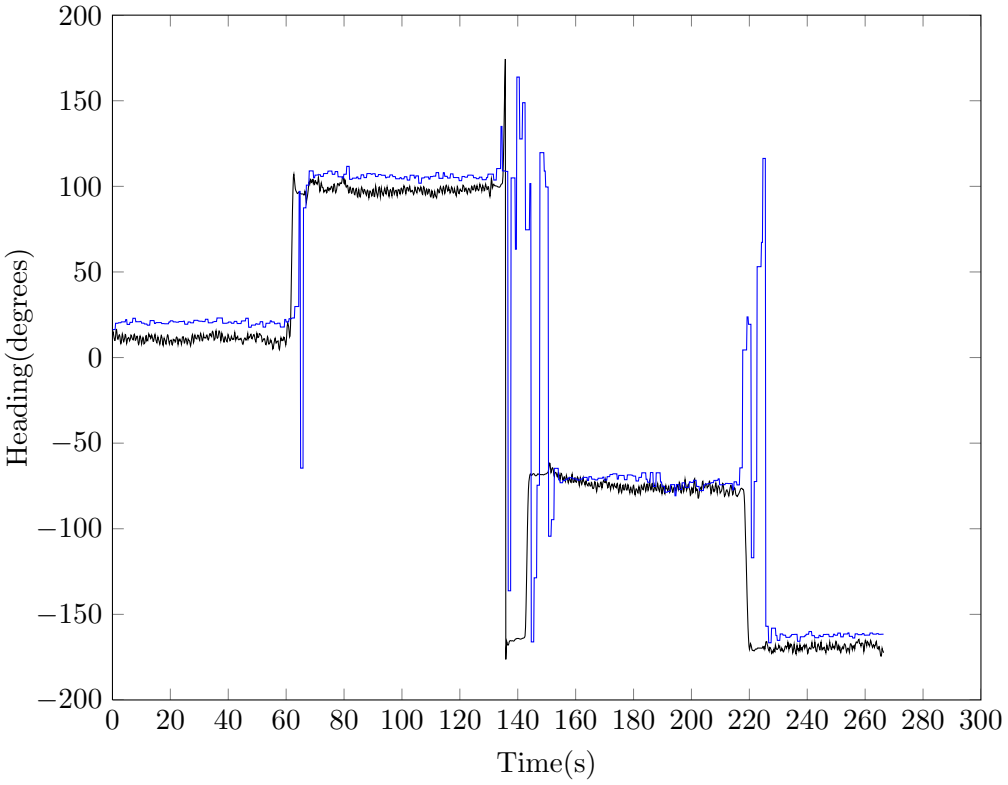

Figure 6.8: The magnetic heading from magnetometer and gyroscope in black and the course from the GPS in blue were used to estimate the magnetic declination.

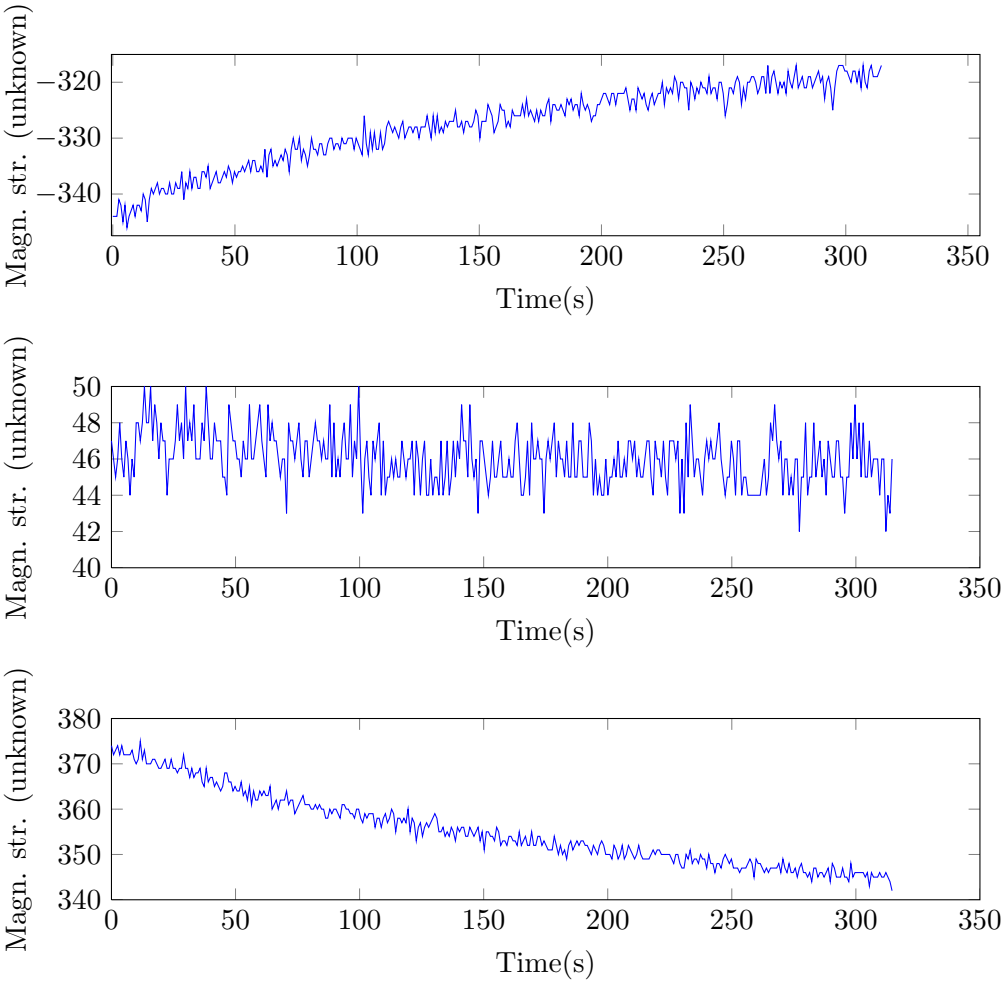

Figure 6.9: The magnetometer measurements for three axes during 5 minutes. The IMU was still during all time.

Chapter 7

Conclusions, Discussion and Further work

Using quaternions for representing the attitude in an EKF worked out well and offered the possibility to very easily redefine the heading when necessary. Decreasing the covariance matrix in the EKF depending on the variance in the accelerometer measurements had the benefit of decreasing the influence of gyroscope drift when standing still or walking calmly. Increasing it when running reduced most of the errors in the amplitude of the heading estimation. The problem with the introduction of error in the attitude estimation caused by changing the influence of the gyroscope was avoided by calculating the value of two other quaternions which were only updated according to the gyroscope in the background. Considering the strength of the measured magnetic field was generally a good indicator of the disturbances on the magnetometer. This method could however not be used when the magnetic field was only disturbed in its strength but not in its direction. In order to be able to handle such situations, another approach was used which is not discussed in this version of the report due to a pending patent.

Estimating the local magnetic declination by comparing the heading from the magnetometer with the course from the GPS was successful and corresponded well to the real value, considering the quality of the sensors used in the project. The calibration routines that were used were simple since they were performed by activities such as placing the IMU on its six sides and by rotating the IMU when placed on a chair. The error models for the calibration were simplified from the complete model, but still fulfilled the purpose of making the measurements from the sensors reliable.

The magnetometer was the cause of most of the problems in this project. One problem discovered was that the calibration constants were different from one logging of data to another and even during the same logging. This fact can be seen in figure 6.9, where the IMU has been lying flat on the ground untouched for about 5 minutes. As can be seen, the measurements varies for the x-axis (top) and z-axis (bottom) almost 10% during this period. An important mean of improvement for further work seems to be to either use better magnetometer, or creating routines for avoiding this time-dependency.

Bibliography

[1] J.F. Vasconcelos, G. Elkaim, C. Silvestre, P. Oliveira and B. Cardeira, "A Geometric Approach to Strapdown Magnetometer Calibration in Sensor Frame" *Navigation, Guidance and Control of Underwater Vehicles*, Volume 2, Part 1

[2] C. C. Foster, G. H. Elkaim UC Santa Cruz, "Extension of a Two-Step Calibration Methodology to Include Nonorthogonal Sensor Axes" *Aerospace and Electronic Systems, IEEE Transactions on (Volume:44 , Issue:3)*, July 2008

[3] A.R. Jimenez, F. Seco, J.C. Prieto and J. Guevara, "Navigation using an INS/EKF framework for Yaw Drift Reduction and a Foot-mounted IMU", *WPNC 2010: 7th Workshop on Positioning, Navigation and Communication 2010.*

[4] I. Skog, P. Händel, Signal Processing Lab, Royal Institute of Technology, Stockholm," Calibration of a mems inertial measurement unit", *XVII Imeko World Congress Metrology for a Sustainable Development September, 1722*, 2006 Rio de Janeiro, Brazil

[5] G. Eriksson,"Numeriska Algoritmer med MATLAB", *NADA, KTH, June 1998*

[6] P. S. Maybeck "Stochastic Models, Estimation, and Control, vol 2.", *New York: Academic Press, 1982*

[7] A. H. Mohamed, K. P. Schwarz "Adaptive Kalman Filtering for INS/GPS Department of Geomatics Engineering", *The University of Calgary,Journal of Geodesy (1999) 73: 193203*

[8] J. R. Vasquez, P. S. Maybeck "Enhanced motion and sizing of bank in Moving-Bank MMAE", *IEEE Transactions on Aerospace and Electronic systems VOL. 40, NO. 3 JULY 2004*

[9] D. A. Karnick, P. S. Maybeck "Moving bank multiple model adaptive estimation" *Proceedings of the 28th Conference on Decision and Control Los Angeles, CA December 1987*

[10] Y. S. Suh, "Orientation estimation using a quaternion-based indirect Kalman filter with adaptive estimation of external acceleration." Instrumentation and Measurement, IEEE Transactions on (Volume:59 , Issue: 12) Dec 2010

[11] Y. S. Suh, S. K. Park, H. J. Kang and Y. S. Ro, "Attitude Estimation Adaptively Compensating External Acceleration" JSME International Journal Series C, Volume 49, Issue 1, pp. 172-179 (2006)

[12] A. M. Sabatini "Quaternion-Based Extended Kalman Filter for Determining Orientation by Inertial and Magnetic Sensing", *IEEE Transaction on biomedical engineering, VOL. 53, NO. 7, JULY 2006*

[13] A. Kim, M.F. Golnaraghi, "A Quaternion-Based Orientation Estimation Algorithm Using an inertial Measurement Unit" Position Location and Navigation Symposium, 2004. PLANS 2004

[14] Y. Li, A. Dempster, B. Li, J. Wang, C. Rizos, "A low-cost attitude heading reference system by combination of GPS and magnetometers and MEMS inertial sensors for mobile applications", *Journal of Global Positioning Systems (2006) Vol. 5, No. 1-2:88-95*

[15] J. A. Rios, Crossbow Technology, Inc, Elecia White, Crossbow Technology, Inc, "Fusion Filter Algorithm Enhancements For a MEMS GPS/IMU" ION NTM 2002

[16] National oceanic and atmospheric administration - National Geophysical data center, http://www.ngdc.noaa.gov/geomag/declination.shtml

[17] J. B. Kuipers, "Quaternions and Rotation sequences", *1999 Princeton University Press, fifth printing, 2002*

[18] B. Palais, R. Palais, and S. Rodi, "A Disorienting Look at Eulers Theorem on the Axis of a Rotation", *The mathematical association of America monthly 116 December 2009*

[19] S. House, S. Connell, I. Milligan, D. Austin, T. L. Hayes, P. Chiang, "Indoor Localization with RFID-Based Fiducials", *33rd Annual International Conference of the IEEE EMBS Boston, Massachusetts USA, August 30 - September 3, 2011*

[20] H. Wang, S. Sen, A. Elgohary, M. Farid, M. Youssef, R. R. Choudhury, "Unsupervised Localization", *MobiSys12, June 2529, 2012, Low Wood Bay, Lake District, UK.*

[21] M. Stamp, "A Revealing Introduction to Hidden Markov Models", September 28, 2012

[22] L. R. Rabiner, "A tutorial on Hidden Markov Models and Selected Applications in Speech Recognition", Proceedings to the IEEE, Vol. 77, NO. 2, February 1989

[23] A. Olivares, G. Olivares, J.M Gorriz, J. Ramirez, High-Efficiency Low-Cost Accelerometer-Aided Gyroscope Calibration, 2009 International Conference on Test and Measurement

[24] F. Gustafsson, L. Ljung, M. Millnert, "Signal Processing", The authors and studentlitteratur 2010, 2010 Edition 1:3